R. & M. No. 3055
(18,331)
(A.R.C. Technical Report)

MINISTRY OF SUPPLY

AERONAUTICAL RESEARCH COUNCIL
REPORTS AND MEMORANDA

A Theoretical and Experimental Investigation of the Flow Over a Family of Rectangular Wings of Biconvex Section at $M = 1 \cdot 42$

By

R. C. Lock, M.A., Ph.D.,
of the Aerodynamics Division, N.P.L.

LONDON: HER MAJESTY'S STATIONERY OFFICE
1958
PRICE 15*s* 0*d* NET

A Theoretical and Experimental Investigation of the Flow Over a Family of Rectangular Wings of Biconvex Section at $M = 1 \cdot 42$

By

R. C. Lock, M.A., Ph.D.,

of the Aerodynamics Division, N.P.L.

Communicated by the Director-General of Scientific Research (Air), Ministry of Supply

Reports and Memoranda No. 3055*

March, 1956

Summary.—An account is given of experiments made at $M = 1 \cdot 42$ using three rectangular half-wing models having biconvex sections with thickness ratios 0·04, 0·06 and 0·08, mounted on a reflection plate. Measurements were made of the pressure on the upper surface of the wing and of pressure and flow direction in the neighbourhood of the wing tip. Direct shadow photography and observation of surface oil patterns enabled various details of the flow to be visualised. The results are correlated with the linearised theory and with certain second-order modifications to this theory. It is found that in general the linearised theory provides a sufficient approximation to the detailed flow only for the thinnest wing at very small incidences. In most cases the suggested modifications effect a considerable improvement.

1. *Introduction.*—The flow in the neighbourhood of the tip of a rectangular wing at supersonic speeds is one of the simplest examples of three-dimensional gas dynamics, and the approximate theoretical solution of the problem by means of the linearised theory, applicable to thin wings at small angles of attack, has been known for some years (*see*, for example, Ref. 1). A considerable amount of experimental evidence is available concerning the overall force characteristics on such wings, and it seems that for wings of moderate aspect ratio the predictions of the linearised theory are substantially verified under the conditions for which they may be expected to apply (*cf.* Ref. 4) ; and by taking approximate account of second-order effects the theory may be extended to cover an increased range of incidence and wing thickness[2]. Much less experimental work seems, however, to have been done on the detailed pressure distribution and flow pattern around rectangular wings (but *see* Refs. 3 and 5), and it was accordingly decided to make a systematic series of tests to investigate the matter more fully, with particular reference to the correlation between theory and experiment. In order to do this three half-wing models were used, of biconvex circular-arc sections having thickness ratios 0·04, 0·06 and 0·08, mounted on a reflection plate. Measurements were made of the surface pressure and of the pressure and flow direction at other points inside the influence region of the wing tip. Standard flow visualisation techniques were used to show certain aspects of the shock-wave pattern round the wings and of the flow over the wing surface.

*Published with permission of the Director, National Physical Laboratory.

2. *Theoretical Work.*—It is convenient at this stage to give a brief account of the most important theoretical information which is at present available on the subject, and to indicate certain extensions which may easily be made. Most of the work is based on the linearised theory, which gives in effect the first approximation to the solution of the exact equations of inviscid flow when these are expanded as an infinite series in powers of the wing thickness ratio or angle of incidence (*see*, for example, Ref. 6). It is well known that, provided the free-stream Mach number M is sufficiently high for the leading-edge shock to be attached and the flow behind it purely supersonic*, then the fact that the wing is cut off at its tips will affect the flow only in certain regions, exterior to which it will be purely two-dimensional in character and can be determined by standard methods. These two 'tip regions' are approximately conical in shape, with the apex of the cones at the extremities of the leading edge; according to the linearised theory they are simply the Mach cones from these points. Provided that the aspect ratio of the wing is greater than a certain value (given by the linearised theory as $2/\sqrt{(M^2-1)}$, these regions will intersect behind the wing trailing edge, so that they may be treated separately as regards the flow in the neighbourhood of the wing; this is the only case which will be considered in the present paper.

2.1. *Linearised Theory.*—Standard rectangular axes are used with origin O at the starboard tip of the wing leading edge, which is referred to as the apex; Ox is taken in the direction of the free stream; Oy horizontally outwards in the spanwise direction (so that y is negative on the wing) and Oz vertically upwards†. The corresponding components of fluid velocity are taken to be $(U+u, v, w)$, where U is the velocity of the undisturbed stream and (u, v, w) are the components of the perturbation velocity. It is convenient to measure x, y and z in terms of the wing chord c, so that the actual spatial co-ordinates are cx, cy and cz.

A wing of symmetrical biconvex section and thickness ratio τ is considered, whose equation at zero incidence is

$$z = \pm 2\tau x(1-x) \quad (0 \leqslant x \leqslant 1, y < 0). \qquad (1)$$

On the assumption of inviscid, irrotational flow, there exists a velocity potential ϕ such that

$$u = \frac{\partial\phi}{\partial x}, \; v = \frac{\partial\phi}{\partial y}, \; w = \frac{\partial\phi}{\partial z},$$

and the linearised equation for steady motion is then

$$B^2\frac{\partial^2\phi}{\partial x^2} - \frac{\partial^2\phi}{\partial y^2} - \frac{\partial^2\phi}{\partial z^2} = 0, \qquad (2)$$

where $B = \sqrt{(M^2-1)}$.

This equation has to be solved under the linearised boundary condition on the wing at incidence α

$$\left.\frac{\partial\phi}{\partial z}\right|_{z=0} = U\{\pm 2\tau(1-2x) - \alpha\}. \qquad (3)$$

Here the alternative signs refer to the upper and lower surfaces respectively. The pressure coefficient will then be given by the equation

$$C_p = \frac{p-p_1}{\frac{1}{2}\rho_1 U^2} = -\frac{2u}{U}$$

to the first order, where p_1 and ρ_1 are respectively the pressure and density of the undisturbed stream.

* The conditions for shock attachment are exactly the same for an unswept wing of finite span as for a two-dimensional wing of the same section.

† In the experiments described in section 4.4, z was in fact measured at all incidences from the mean plane of the wing; this does not affect the linearised theory but has been taken into account in the second-order calculations where necessary.

According to the linearised theory the effects of thickness and incidence may be treated separately, and the results then added to give the flow at incidence over a wing of finite thickness. At zero incidence the flow is equivalent to that produced by a distribution of supersonic sources over that part of the plane $z = 0$ occupied by the wing, of strength proportional to the slope $2\tau(1 - 2x)$ of the surface ; it is thus a straight forward matter to calculate the pressure and velocity at any point. The additional flow due to incidence is conical, so that the problem may be reduced to a two-dimensional one and solved by one of the standard methods for conical flows (*see* Refs. 6 and 7). These methods make use of conical co-ordinates y_1, z_1, r and θ defined by

$$y_1 = By/x = r\cos\theta$$
$$z_1 = Bz/x = r\sin\theta\ ,$$

so that $r = B\sqrt{(y^2 + z^2)}/x$

and $\theta = \tan^{-1}(z/y)$.

Thus $\theta = \pi$ on the upper surface of the wing where y is negative.

The following expressions are finally obtained for the components of the perturbation velocity and the pressure coefficient, for a wing of thickness ratio τ at incidence α, in the region bounded by the Mach cone from the apex O and the envelope of the Mach cones from points on the trailing edge ; details of their derivation are given in the Appendix.

$$\frac{u}{U} = -\tfrac{1}{2}C_p = \frac{\alpha}{\pi B}\cos^{-1}\frac{1 - r + y_1}{\sqrt{(1 - z_1^2)}}\operatorname{sgn} z - \frac{2\tau}{\pi}\times$$

$$\times\left[\frac{1}{B}(1 - 2x)\cos^{-1}\frac{y_1}{\sqrt{(1 - z_1^2)}} + 2|z|\cos^{-1}\frac{y_1}{r\sqrt{(1 - z_1^2)}} + 2y\cosh^{-1}\frac{1}{r}\right], \quad (4)$$

$$\frac{v}{U} = -\frac{2\alpha}{\pi}\sqrt{\left(\frac{1 - r}{r}\right)}\sin\tfrac{1}{2}\theta + \frac{2\tau}{\pi}\left[2x\sqrt{(1 - r^2)} + (1 - 2x)\cosh^{-1}\frac{1}{r}\right] \quad (5)$$

and

$$\frac{w}{U} = \frac{2\alpha}{\pi}\left[\sqrt{\left(\frac{1 - r}{r}\right)}\cos\tfrac{1}{2}\theta + \tfrac{1}{2}\cos^{-1}\frac{1 - r - y_1}{\sqrt{(1 - z_1^2)}} - \frac{\pi}{2}\right]$$

$$+ \frac{2\tau}{\pi}\operatorname{sgn} z\left[(1 - 2x)\cos^{-1}\frac{y_1}{r\sqrt{(1 - z_1^2)}} + 2B|z|\cos^{-1}\frac{y_1}{\sqrt{(1 - z_1^2)}}\right]. \quad (6)$$

Here the value of the inverse cosine between 0 and π is to be taken (Equations (4), (5) and (6) in their complete form do not appear to have been derived previously, though the results when $\tau = 0$ are given by Lagerstrom and Graham[8]).

In the plane of the wing, where $z = 0$, these equations simplify to give the following well-known results

$$\frac{u}{U} = \pm\frac{\alpha}{\pi B}\cos^{-1}(1 - |y_1| + y_1) - \frac{2\tau}{\pi}\left[\frac{1}{B}(1 - 2x)\cos^{-1}y_1 + 2y\cosh^{-1}\frac{1}{|y_1|}\right], \quad (7)$$

$$\frac{v}{U} = \mp\frac{2\alpha}{\pi}\sqrt{\left(\frac{1 - |y_1|}{|y_1|}\right)}H(-y_1) + \frac{2\tau}{\pi}\left[2x\sqrt{(1 - y_1^2)} + (1 - 2x)\cosh^{-1}\frac{1}{|y_1|}\right] \quad (8)$$

and

$$\frac{w}{U} = \frac{2\alpha}{\pi}\left[\sqrt{\left(\frac{1 - |y_1|}{|y_1|}\right)}H(y_1) + \tfrac{1}{2}\cos^{-1}(1 - |y_1| - y_1) - \frac{\pi}{2}\right] \pm \frac{2\tau}{\pi}(1 - 2x)\cos^{-1}\frac{y_1}{|y_1|}. \quad (9)$$

Here the alternative signs refer to the upper and lower surfaces respectively and $H(y_1)$ is the standard ' unit function ' defined by

$$H(y_1) = \begin{cases} 1 \text{ if } y_1 > 0 \,, \\ 0 \text{ if } y_1 < 0 \,. \end{cases}$$

Outside the Mach cone $r = 1$ the flow is two-dimensional in character, and the perturbation velocities are either zero (outside the influence region of the wing) or given by

$$\frac{u}{U} = \pm \frac{\alpha}{B} - \frac{2\tau}{B}\{1 - 2\,(x \mp Bz)\}\,,$$

$$v = 0$$

and

$$\frac{w}{U} = -\,\alpha \pm 2\tau\{1 - 2(x \mp Bz)\}.$$

By the use of these equations, calculations have been made of the following quantities, for wings with $\tau = 0{\cdot}04$, $0{\cdot}06$ and $0{\cdot}08$, over a range of incidence at $M = \sqrt{2}$:

C_p on the upper surface of the wing along the lines $\psi = 15$, 30, 38 and 48 deg, where $\psi = \tan^{-1}(-y_1)$

C_p, v/U and w/U along the lines $z = 0 (y > 0)$, $y = 0 (z > 0)$ and $z = \frac{1}{4}$, in the plane $x = \frac{1}{2}$. The results of these calculations are shown in Figs. 3 to 14, where they are compared with the corresponding experimental values.

All the preceding equations apply only upstream of the region which is influenced by the vortex wake of the wing, bounded by the envelope of Mach cones from the trailing edge. In this region the flow at zero incidence presents no difficulty, though the formulae given above have to be modified to allow for the vanishing of the source strength in the plane of the wing downstream from the trailing edge. But the flow due to incidence is radically altered ; the lifting surface treated in conical-flow theory is replaced by a vortex sheet, whose strength is constant in a streamwise direction, extending downstream from the trailing edge, and across which the pressure must be continuous and equal to the free-stream pressure. The flow is clearly no longer conical ; but Lagerstrom and Graham[8] have shown that it may be represented by the superposition of an infinite number of conical fields, originating from every point on the trailing edge which lies inside the Mach cone from the apex. Details will not be given here, since no experimental measurements were made in this region ; but it is interesting to consider what happens in the wake just downstream of the trailing edge, and this may be found by the following simple argument, also due to Lagerstrom and Graham[8]. In passing from the upper or lower surface of the wing into the wake, the flow is deflected at the trailing edge by means of a shock or centred expansion wave in such a way that the pressure just downstream of the trailing edge is the same for fluid coming from either surface. Now the pressure change across a weak oblique shock or expansion is related to the flow deflection δ by the equation $\Delta C_p = 2\delta/B$ to the first order. If the wing incidence is α, the trailing edge angle 2λ and the downwash angle ε, then the flow deflections for the upper and lower surfaces are $\lambda \pm (\alpha - \varepsilon)$ respectively, so that $\lambda + \alpha - \varepsilon = \frac{1}{2}B(C_{pW} - C_{pU})$ and $\lambda - \alpha + \varepsilon = \frac{1}{2}B(C_{pW} - C_{pL})$, where the suffices U, L and W denote values at the trailing edge on the upper and lower surfaces and in the wake respectively.

Therefore

$$\varepsilon = \alpha + \tfrac{1}{4}B(C_{pU} - C_{pL})$$

$$= \alpha\left[1 - \frac{1}{\pi}\cos^{-1}(1 + 2y_1)\right](-1 \leqslant y_1 \leqslant 0) \qquad .. \quad .. \quad .. \quad (10)$$

and

$$C_{pW} = C_{pU} + \frac{2}{B}\left[\lambda + \frac{\alpha}{\pi}\cos^{-1}(1 + 2y_1)\right](-1 \leqslant y_1 \leqslant 0) \qquad .. \quad .. \quad (11)$$

for any symmetrical wing ; in the present case $\lambda = 2\tau$. The downwash angle ε calculated from equation (10) is plotted in Fig. 19 ; it will be seen that ε increases steadily from zero behind the two-dimensional region to the value α behind the wing tip. It should however be pointed out that the above theory depends on the sidewash v/U being small, and this is clearly not true very near the wing tip.

2.2. *Higher-Order Theories.*—2.2.1.—In the region where the flow is two-dimensional (the shape of the boundaries of this region is discussed below), the Busemann second-order theory may be used, and moreover the pressure on the surface of the wing may be found with considerable accuracy in the absence of viscous effects by means of the shock-expansion theory (*cf.* Lighthill, Ref. 9), provided that the leading edge shock is attached.

It is interesting to note that, even if the incidence is so great that the deflection onto the lower surface is large enough to cause this shock to detach, it is still possible formally to work out the shock-expansion theory for the upper surface as if shock detachment had not occurred. The results will certainly be in error near the leading edge but may nevertheless be reliable except in this region, as indeed proves to be the case.

The pressure distributions calculated in this way are shown in Figs. 3 to 5 as ' simple shock-expansion theory ' for $\psi = 48$ deg.

2.2.2.—When the flow is truly three-dimensional, there has been as yet little progress in extending the linearised theory to higher approximations. Such progress that has been made may be divided into two parts : first, rigorous investigations into the nature of the flow near the Mach cone from the apex and in particular into the shape of the nearly conical shock from this point ; and second, simple non-rigorous methods designed to improve the accuracy of estimation of the pressure distribution and forces on the wing surface.

Lighthill[11, 12] has shown that in the neighbourhood of the Mach cone $r = 1$ the series solution to the exact equations of inviscid flow, of which the linearised solution represents the first term, is not uniformly convergent and that therefore the linearised theory does not give correctly even a first approximation to the flow in this region. This difficulty may be avoided by expanding the co-ordinate r, as well as the perturbation velocity potential ϕ, as an infinite series in powers of a small quantity ε representing the thickness ratio or angle of incidence ; thus

$$r = R + \sum_{n=1}^{\infty} \varepsilon^n r_n (\theta, x, R)$$

and

$$\phi = \sum_{n=1}^{\infty} \varepsilon^n \phi_n(\theta, x, R) .$$

The correct first approximation $\varepsilon \phi$, (θ, x, R) to the velocity potential ϕ near $r = 1$ is thus found by substituting R for r in the expression $\varepsilon \phi$, (θ, x, r) given by the ordinary linearised theory ; the function r, which expresses to the first order the difference between r and R has to be found from second-order considerations, taking into account the conditions which must be satisfied across the shock. In this way Lighthill[12] has obtained first approximations to the strength and position of the shock in certain problems of conical flow, in particular that of a rectangular flat plate at incidence. For a wing of finite thickness the flow is not strictly conical, so that Lighthill's results cannot be applied directly, but some insight into the actual flow pattern near the Mach cone may be obtained by considering the related conical problem of flow over a rectangular wedge.

For a wedge of semi-angle δ at incidence α, the pressure is given by

$$\frac{p - p_1}{\rho_1 U^2} = \frac{\delta}{\pi B} \cos^{-1} \frac{y_1}{\sqrt{(1 - z_1^2)}} - \frac{\alpha}{\pi B} \cos^{-1} \frac{1 - r + y_1}{\sqrt{(1 - z_1^2)}} \operatorname{sgn} z ,$$

in the notation of 2.1. Near the Mach cone $r = 1$ it is found that

$$\frac{p - p_1}{\rho_1 U^2} \sim \frac{1}{B}(\delta - \alpha \operatorname{sgn} z) H(-y_1) + A(\theta)\sqrt{(1 - r)},$$

where $$A(\theta) = \frac{\sec\theta\sqrt{2}}{\pi B}(\delta - \sqrt{(2)}\,\alpha \sin\tfrac{1}{2}\theta)\,. \quad .. \quad .. \quad .. \quad .. \quad .. \quad (14)$$

Lighthill[12] has shown that the strength and displacement of the shock from the Mach cone are both proportional to the square of the strength $A(\theta)$ of the singularity in the linearised theory, provided that this is *positive*.

Thus, whenever $A(\theta) > 0$, a shock exists of strength given by

$$\Delta C_p = \frac{3}{2}(\gamma + 1)\frac{M^4}{M^2 - 1}A^2(\theta) \quad .. \quad .. \quad .. \quad .. \quad .. \quad .. \quad (15)$$

lying (for $y > 0$ only) on the cone

$$r = 1 + \frac{3}{16}(\gamma + 1)^2 \frac{M^8}{(M^2 - 1)^2}A^2(\theta)\,. \quad .. \quad .. \quad .. \quad .. \quad .. \quad (16)$$

If $A(\theta)$ is *negative* (corresponding to an expansion as the Mach cone is crossed in a streamwise direction), then both the shock strength and (for $y > 0$) displacement from the Mach cone are of lower order. An additional singularity occurs along the lines in which the conical shock surface meets the plane shock from the leading edge ; the above results break down in these regions.

We see from equation (14) that if $|\alpha| \leqslant \delta/\sqrt{2}$ then $A(\theta)$ has the same sign as $\cos\theta$, so that there is a shock outboard of the wing tip ($y > 0$) and an expansion inboard ($y < 0$). For greater values of $|\alpha|$ this is still true below the wing at positive incidence, but above the wing the situation is reversed whenever $\pi \geqslant \theta \geqslant 2\sin^{-1}\{\delta/(\alpha\sqrt{2})\}$. The nature of the shocks is shown diagrammatically for various values of α in Fig. 18.

For flow over a finite closed wing the above results are no longer strictly applicable, except in the immediate neighbourhood of the leading edge, where the wedge semi-angle δ must be replaced by half the leading-edge angle ; thus $\delta = 2\tau$ in the present case. However, it may easily be shown that, according to the linearised theory, the singular part of the pressure near the Mach cone $r = 1$ is still $\rho_1 U^2 A(\theta)\sqrt{(1 - r)}$, with $A(\theta)$ given by equation (14) ; so that it seems probable that the correct first approximations to the shock strength and position are still given by equations (15) and (16) (where applicable), provided that the distance from the leading edge is not too great. Further downstream it is well known that the shocks decay in strength and that the inclination of the shock surfaces decreases steadily towards the free-stream Mach angle.

It remains to consider the shape of the surface separating the two-dimensional flow over the wing from the tip region ; note that equation (16) does not apply here. Since it is known that the strength of any shocks which may be present is at most of the second order in τ or α, it follows that to the first order this surface must be an envelope of characteristics of the two-dimensional flow, and this makes it possible to determine its shape.

Suppose that the equation of the surface is

$$r = 1 + f(\theta, x)\,, \quad .. \quad .. \quad .. \quad .. \quad .. \quad .. \quad .. \quad .. \quad (17)$$

where f is of the first order in τ and α. The condition that equation (17) should represent a characteristic surface of the neighbouring two-dimensional flow is that the angle between the normal to (17) and the local flow direction should be $\pi/2 \pm \mu$, where μ is the local Mach angle. Now, for two-dimensional flow above an aerofoil whose upper surface has the equation $z = Z(x)$

at zero incidence, the velocity vector has direction cosines $(1, 0, \zeta(x - Bz))$ correct to $0(\tau)$, where $\zeta(x) = Z'(x) - \alpha$ is the local inclination of the surface, and the local Mach angle is given by

$$\sin \mu = \frac{1}{M}\left[1 + \frac{\{1 + \frac{1}{2}(\gamma - 1)M^2\}}{B}\zeta(x - Bz)\right].$$

The relevant direction cosines of the normal to (17) can be shown to be

$$l = -\frac{1}{M}\left\{1 + \frac{B^2}{M^2}\left(f + x\frac{\partial f}{\partial x}\right)\right\} + 0(\tau^2)$$

and

$$n = \frac{B}{M}\sin\theta + 0(\tau),$$

so that the condition mentioned above leads to the relation

$$\frac{B^2}{M^2}\frac{\partial}{\partial x}(xf) = \left[B\sin\theta + \frac{\{1 + \frac{1}{2}(\gamma - 1)M^2\}}{B}\right]\zeta(x - Bz). \quad \ldots \quad \ldots \quad \ldots \quad (18)$$

This equation has to be satisfied near the Mach cone, where $Bz \simeq x\sin\theta$, so that it may be integrated directly to give, as the final form for equation (17)

$$r = 1 + \frac{M^2}{B^3}[(M^2 - 1)\sin\theta + \{1 + \tfrac{1}{2}(\gamma - 1)M^2\}]\left\{\frac{1}{\zeta}Z(\xi) - \alpha\right\}\left(\frac{\pi}{2} \leqslant \theta \leqslant \pi\right), \quad (19)$$

where $\xi = x(1 - \sin\theta)$. A similar result can be obtained in the range $-\pi \leqslant \theta \leqslant -\pi/2$.

In the present case $Z(x) = 2\tau x(1 - x)$, so that equation (19) becomes

$$r = 1 + (M^2/B^3)\{(M^2 - 1)\sin\theta + 1 + \tfrac{1}{2}(\gamma - 1)M^2\} \times \times \{2\tau(1 - x + x\sin\theta) - \alpha\}. \quad \ldots \quad \ldots \quad \ldots \quad (20)$$

The corresponding result when $\tau = 0$ has been obtained in a different way by Lighthill[12].

The theory given above is applicable (to the first order) whether or not a shock of second-order strength exists on the surface under consideration. When there is no second-order shock, *i.e.*, when $A(\theta)$ is negative, a higher approximation to the shape of the dividing surface could be obtained in a similar way, using the Busemann second-order theory for the two-dimensional flow. In cases where a shock is present, no further progress can be made without knowledge of the complete second-order solution.

2.2.3.—Though a true second-order solution for the flow in the tip region has not yet been obtained (but *see* Ref. 13), an attempt has been made by Czarnecki and Mueller[5] to modify the pressure distribution on the wing surface obtained by means of the linearised theory so as to give better agreement with experiment. In its simplest form their method may be described briefly as follows :

The pressure distribution for a two-dimensional aerofoil of the same section is first calculated by the shock-expansion method, at zero incidence and at the required incidence α. The pressure coefficients obtained in this way are written as the sum of their value at zero incidence and an increment due to incidence ; thus $C_p(x) = C_{p,0}(x) + C_{p,\alpha}(x)$. To find the pressure coefficient at a point (x, y) on the surface in the tip region, we take

$$C_p(x, y) = F_1(x, y)\, C_{p,0}(x) + F_2(x, y)\, C_{p,\alpha}(x), \quad \ldots \quad \ldots \quad \ldots \quad \ldots \quad \ldots \quad (21)$$

where $F_1(x, y)$ is the ratio of the pressure coefficient at the point (x, y) to that at a point with the same value of x in the two-dimensional region, according to the linearised theory for $\alpha = 0$; $F_2(x, y)$ is similarly defined from the linearised theory of the flow due to incidence. Some results of this simple method are shown in Figs. 3 to 5 as ' simple shock-expansion theory '.

The method can be refined to allow for the fact that the region of the wing surface influenced by the tip is not in fact bounded by a straight Mach line from 0, but by a curve which, as discussed in the previous section, is at least to the first order a characteristic of the two-dimensional flow and is therefore given approximately by the equation

$$-y = Y(x) = \int_0^x \frac{dx}{\sqrt{\{M^2(x) - 1\}}} \quad \ldots \ldots \ldots \ldots \ldots \ldots \quad (22)$$

Here $M(x)$ is the local Mach number as calculated by the shock-expansion method. Czarnecki and Mueller therefore suggest that the functions F_1 and F_2 of equation (21) should be evaluated, not at the point (x, y) at which the value of C_p is desired, but at a point (x', y') displaced to allow for the distortion of the tip region. They give various methods of doing this, the simplest of which consists of linear distortion in the spanwise direction. Thus we take

$$x' = x,$$

$$y' = y \frac{x}{BY(x)}.$$

The results of this modification are shown in Figs. 3 to 5 as ' modified shock-expansion theory '.

3. *Experimental Details.*—3.1. *The Tunnel and Reflection Plate.*—The tests described below were made in the 18-in. × 14-in. High-Speed Wind Tunnel at the National Physical Laboratory, using supersonic liners designed to give a nominal Mach number of 1·4. All models were mounted on a reflection plate fixed to the tunnel wall, in order to bypass the wall boundary layer. The plan-form of the reflection plate (*see* Fig. 2) was designed according to the principles described by Ormerod[14], in particular the angle of inclination to the flow of the leading edges (60 deg) was chosen so that they would remain supersonic throughout a model incidence range of ± 15 deg at the Mach number of the tests. In fact preliminary tests showed that the disturbance caused by the plate leading edges did not noticeably increase in magnitude up to an incidence of 20 deg. The plate was mounted on the turntable in the tunnel wall by three struts so as to provide a clearance of 2 in. from the plane of the wall ; directly behind the plate the turntable was hollowed out in order to compensate for the additional blockage due to the plate and its supports.

A thorough preliminary calibration was made of the test region, including measurements of static pressure and flow direction. It was found that the mean Mach number was 1·42 with an overall variation of ± 0·02 ; in the region influenced by the wing tip, of particular interest in the present tests, the variation was not greater than ± 0·01. The flow direction varied in yaw between ± 0·4 deg and in pitch between ± 0·2 deg ; again the variation was less in the tip region. The principal cause of non-uniformity in the flow appeared to be not the reflection plate but a vertical window junction in the opposite wall of the tunnel, which produced a weak shock crossing the plane of the wing just inboard of the Mach line from the tip leading edge ; this probably did not interfere seriously with flow measurements inside the tip region of the wings, but caused difficulty in determining the shape and nature of the inboard boundary to this region. The use of the reflection plate made it inadvisable to attempt any flow measurements downstream of the wing trailing edge, since the strong compression between the plate and the tunnel wall propagated even upstream of the rear end of the plate, causing a rapid fall in Mach number about 1 in. downstream of the wing trailing-edge position at all spanwise stations.

3.2. *The Models.*—Three half-wing models were used, each of rectangular plan-form with 3-in. chord and 4-in. span, giving an effective aspect ratio of $2\frac{2}{3}$, and having symmetrical biconvex circular-arc sections of thickness/chord ratios 0·04, 0·06 and 0·08 respectively ; the wing tips were cut off square. A flange at the base of the wing fitted into a slot in the reflection plate, and was connected to the turntable on the tunnel wall by means of a hollow circular cylinder, which also served to transmit the tubes from the pressure holes ; thus the model and reflection plate both rotated with the turntable. The upper surface of each wing was provided with 21

pressure holes of about 0·01 in. diameter, arranged as far as possible along rays from the apex making angles 15 deg, 30 deg, 38 deg and 48 deg with the tip chord line (*see* Fig. 1) ; one hole was also provided on the lower surface to check the position of zero incidence. Owing to the small thickness of the models only seven tubes could be provided for transmitting the pressures, so that holes not in use had to be sealed. Several methods of doing this were tried ; the most successful consisted of applying a thin film of cellulose nitrate dissolved in acetone over the top of the hole. Optical tests showed that the maximum thickness of the film never exceeded 0·0003 in., so that no interference with the flow need be feared.

All tests were made with the boundary layer on the upper surface turbulent, transition being fixed by means of a band of aluminium paint mixed with carborundum grains extending over about 6 per cent chord from the leading edge. The standard sublimation technique, using hexachlorethane, was employed to verify that this band was efficacious in causing transition.

3.3. *Details of Tests.*—During most of the experiment the stagnation pressure was held constant at 31 in. mercury absolute, giving a Reynolds number $1{\cdot}2 \times 10^6$ based on the wing chord. No tests were made at higher Reynolds numbers, but it is thought that the scale effect with turbulent boundary layers is likely to be very small (*cf.* Ref. 16).

Measurements of pressure on the upper surface of the three wings were made over a range of incidence from -5 deg to 13 deg or 15 deg ; the upper limit, being the maximum obtainable at this Mach number due to tunnel blockage, varied to a certain extent with the thickness of the model. Repeat measurements were taken in most cases. Comparison of the results obtained from holes at the same relative position on the upper and lower surfaces showed that the error in the measured incidences at small lift coefficients did not exceed about 0·1 deg. At high incidences the lift on the thinnest wing caused a considerable deflection of the tip. Observations by means of an incidence telescope showed that the vertical deflection rose to about 0·1 in. at $\alpha = 13$ deg, but that the twist was never greater than about 0·15 deg. No correction has therefore been applied to the measurements of wing incidence.

The following procedure was adopted in reducing the results to the form of pressure coefficients. For each pressure hole, the measured pressure was plotted against incidence and a mean curve drawn, using the results of all repeat measurements. From this curve was subtracted the value of the pressure measured at the corresponding point in the empty tunnel, and the corrected pressure coefficients were then obtained in the usual way. These pressure coefficients are plotted against chordwise position x along the lines $\psi = 15$, 30, 38 and 48 deg in Figs. 3, 4 and 5 for $\tau = 0{\cdot}04$, 0·06 and 0·08 respectively ; the results of the theoretical calculations described in section 2 are also shown.

In addition to these measurements of surface pressure, a detailed investigation was made of the flow in the vertical plane through the half-chord line of the wings (the plane $x = \frac{1}{2}$). Pressures were measured by a standard supersonic static probe of 0·08 in. outside diameter, and the direction of flow was obtained by means of a Conrad-type yaw-meter having two parallel total-head tubes, each of 0·06 in. diameter, cut off at the tip in the form of a wedge of 60 deg total angle ; separate measurements had to be made of the flow direction in horizontal and vertical planes. The sensitivity of this yaw-meter at $M = 1{\cdot}4$ was found to be 10·0 in. of water per degree.

In all cases a correction was applied, as for the surface pressure measurements, by subtracting the value of the appropriate quantity measured at the corresponding point in the empty tunnel. It was found difficult to repeat accurately the exact alignment of the yaw-meter at zero incidence ; consequently all traverses were started outside the influence region of the wing, to provide an absolute comparison with the empty tunnel results.

Traverses were made along three lines in the plane $x = \frac{1}{2}$; horizontally along the wing half-chord line ($z = 0$), vertically above the wing tip ($y = 0$) and horizontally along a line $\frac{3}{4}$ in. above the wing half-chord line ($z = \frac{1}{4}$). The results are shown in Figs. 6 to 14, where the theoretical calculations described in section 2 are also given.

3.4. *Flow Visualisation.*—The use of an opaque reflection plate for mounting the models made it impossible to use standard direct shadow or schlieren methods, but by coating the plate with white paint and illuminating it with a normally incident beam of parallel light it was found that a shadow pattern could be obtained of sufficient clarity to enable good photographs to be taken. In this way it was possible to see the principal details of the overall shock pattern and of the wake, though little could be distinguished of the boundary layer on the wing. Photographs of these shadow patterns over a range of incidence are shown in Fig. 16.

In order to visualize the flow pattern on the wing surface, experiments were made using a thin coating of a mixture of titanium oxide and heavy oil applied uniformly to the upper surface of the wing. Reasonably clear oil patterns were obtained at high incidences after a few seconds running time*. Photographs of these oil patterns are shown in Fig. 17 ; they were taken while the tunnel was running to avoid the distortion which resulted when the tunnel shock passed over the model in shutting down.

4. *Discussion of Results.*—4.1. *The Pressure Distribution on the Wing Surface.*—In Figs. 3, 4 and 5 the experimental pressure distributions on the upper surface are compared with the results of the linearised theory (equation (7)) and of the simple and modified shock-expansion theories described in section 2.2.3. It can be seen that in general the approximation provided by the linearised theory is reasonably adequate only for the thinnest (4 per cent) wing at small positive angles of incidence, and becomes steadily worse as the incidence or thickness is increased, particularly at negative incidences.

The simple shock-expansion theory gives results which are in good agreement with experiment (having regard to the possible experimental error, which may reach $\pm 0{\cdot}01$ on C_p) for all three wings over a wide range of positive incidences (up to 8 deg and in some cases even to 12 deg), except near the wing tip ($\psi = 15$ deg) and, at low incidences, along the line $\phi = 48$ deg. The modification suggested by Czarnecki and Mueller to take into account the distortion of the tip region due to finite incidence and thickness (' modified shock-expansion theory ') seems, at least in the present case, inferior to the simple shock-expansion theory where the two differ significantly, except at low incidences along the line $\psi = 48$ deg ; and even here the effect of the distortion appears to be overestimated. It should, however, be remembered that this modification was designed primarily to take into account the effect of thickness and would certainly not be applicable at incidences high enough to cause the leading-edge shock to detach† ; indeed the remarkably good results given at such incidences by the simple shock-expansion theory must be regarded as to some extent fortuitous.

Some insight into the range of validity of these theories may be gained from consideration of the degree to which the tip region is distorted from the simple Mach triangle $0 \leqslant -y_1 \leqslant 1$. The boundary to this region may be found from equation (22), on the assumption that it is approximately a characteristic of the neighbouring two-dimensional flow, as described in sections 2.2.2 and 2.2.3. This assumption is not strictly valid either when a shock occurs at the boundary between the two regions§ or when the leading-edge shock is detached, but may nevertheless provide a useful guide even in these cases. The results of these calculations are shown in Fig. 15. It is seen that for values of α between about 4 deg and 8 deg the distortion is of the nature of a contraction and, except near the leading edge, is almost independent of wing thickness. For smaller positive incidences the distortion is very small for the thinnest wing but changes rapidly as the thickness is increased ; thus for the thickest wing at zero incidence there is a large extension of the tip region. Even for the thinnest wing this extension becomes large at quite small negative

*Subsequent experience has indicated that better results could have been achieved by using an even thinner layer of oil.

†The incidences at which the shock detaches are $\pm 5{\cdot}4$, $\pm 3{\cdot}1$ and $\pm 0{\cdot}8$ deg for the three aerofoils in order of increasing thickness.

§According to the linearised theory (*cf.* equation (14)) this happens when $\alpha \geqslant \tau\sqrt{2}$; initial values for the three wings in ascending order of thickness are $\alpha = 3{\cdot}2$, $4{\cdot}8$ and $6{\cdot}4$ deg.

incidences, due to the strong leading-edge shock, and for the two thicker wings at $\alpha = -4$ deg the existence of an appreciable subsonic region behind the detached leading-edge shock means that the tip region is effectively unbounded.

This explains why none of the theories quoted above give acceptable results at negative incidences at the comparatively low supersonic Mach number of the present tests. It appears also that the Czarnecki-Mueller modification is reliable when the distortion of the tip region consists chiefly of an extension (provided this is not too large) but should not be used when a contraction occurs. No explanation can be offered ; but it is perhaps worth noting that it is in the latter case that a shock is liable to occur at the boundary between the tip and two-dimensional regions.

A further point of interest concerns the nature of the flow in the immediate vicinity of the wing tip. A study of the pressure curves for $\psi = 15$ deg (Figs. 3a, 4a and 5a) at high incidences shows that the experimental pressures are in most cases considerably lower than those predicted by the simple shock-expansion theory, which gives good results further inboard ; for the thinnest wing they are indeed even below the linearised theory (Fig. 3a, $\alpha = 12$ deg), though the effect becomes less marked as the wing thickness is increased. This can be explained in terms of the theoretical singularity which exists at the wing tip ; for a real flow this leads at moderate incidences to flow separation from the edge of the upper surface of the wing, thus producing a region of concentrated vorticity just above the tip.

The phenomenon of tip separation has been studied theoretically by several writers, particularly at low speeds, and it is well established that the resulting vorticity leads to an increase of suction on the upper surface of the wing near the tip, as has been observed in the present experiments. Cheng[16] has given a theoretical treatment of the supersonic flow past a rectangular flat plate and has calculated the change in pressure distribution due to the tip separation ; but his simple model of the flow is to some extent unrealistic in that it assumes a discrete conical vortex without the physically necessary feeding vortex sheet and thus overestimates the magnitude of the effect, a defect which is shared by the similar methods of Edwards[17], Adams[18] and Brown and Michael[19] for thin delta wings. Furthermore, it is clear that for a wing of finite thickness the phenomenon will be sensitive to the shape of the wing tip, but if a reliable theory were available for the flat plate it might be extended by applying it only from that incidence at which separation was first observed, as suggested by Küchemann[20].

It should be emphasized that for finite wings the effect is essentially of the second order, at least as regards the detailed pressure distribution, as may be seen from the fact that in only one case (for the thinnest wing at incidences above about 10 deg) is the suction actually greater than that predicted by linearised theory. Thus any theoretical attempts to correct for tip separation must start from a reliable second-order theory of the unseparated flow, when this becomes available.

4.2. *Surface Flow Patterns.*—The surface oil patterns which were obtained at high incidences (Fig. 17) are also of interest in this connection, since they show clear traces of tip separation and in many cases of the characteristic outflow near the tips which is associated with the presence of a vortex lying above the surface.

Many of these photographs also show the position of the shock wave which forms the inboard boundary to the tip region, marked by an abrupt change in direction of the surface streamlines as they cross the shock. The shock positions seem to be in qualitative agreement with the theoretical ideas mentioned previously (Fig. 15) ; they lie in all cases well within the tip Mach cone, and there are signs of the predicted contraction of the tip region with increasing incidence.

The extent of flow separation near the trailing edge can be clearly seen by this method. In interpreting the results it is important to bear in mind the work of Gadd and Holder (Refs. 21 and 22) on boundary-layer separation induced by oblique shocks. They have shown that, for turbulent boundary layers at local Mach numbers above 1·5, an appreciable amount of separation may be expected if the flow deflection through the shock exceeds about 12 deg ; this criterion

has been confirmed by some experiments on a double-wedge aerofoil at $M = 1{\cdot}6$[23]. Thus two-dimensional trailing-edge separation would be expected for the present series of aerofoils at incidences exceeding about 8, 5 and 3 deg respectively. The photographs show in all cases a considerable amount of separation at the junction of the trailing edge with the reflection plate, due to the interaction there of the two boundary layers ; if this effect is ignored and attention is concentrated on the edge of the tip region (about $\frac{1}{4}$ span outboard from the plate), it is seen that the degree of separation is consistent with the above figures. Thus for the 4 per cent thick wing there is a small amount of separation at $\alpha = 10$ deg, for the 6 per cent wing the separation at this incidence is considerably greater, and the 8 per cent wing shows an appreciable separation at $\alpha = 8$ deg. As the incidence is increased the separation in this region also increases rapidly, partly due to interaction between the trailing-edge shock and the two conical shocks springing from the tip and root of the leading edge. Outboard of this region there is a marked decrease in the amount of separation, which in no case extends as far as the tip of the trailing edge. This is due largely to the rapid increase in downwash as the trailing edge is approached (*see* Fig. 19) ; thus at the tip itself the linearised theory predicts that the downwash angle is exactly equal to the angle of incidence so that, according to Gadd's criterion, there should be no change in separation with incidence, as indeed appears to be the case.

The effect of trailing-edge separation can of course also be seen in the local loss of suction at high incidences, notably from the pressure distributions along the line $\psi = 38$ deg (Figs. 3c, 4c and 5c) and to a lesser degree along the line $\psi = 30$ deg (Figs. 4b and 5b) ; the lack of a pressure hole near the trailing edge on the line $\psi = 48$ deg prevents observation of the even more marked effect which must have occurred along this line.

4.3. *Direct Shadow Photographs.*—The most interesting feature of the direct shadow photographs (Fig. 16) is the double trailing-edge shock which is visible at low incidence on both surfaces. This can be explained very simply in terms of the shape of the trailing-edge shock surface. Consider, for example, the flow at zero incidence. In the two-dimensional region the local Mach number at the trailing edge is higher than that of the free stream and the inclination of the shock to the free-stream direction is less than the Mach angle of the undisturbed flow. As the tip region is entered the local Mach number decreases and so the inclination of the shock increases, reaching a maximum near the tip where it verges into the weaker conical shock from the extremity of the trailing edge.

On the assumptions of the linearised theory the shape of the trailing-edge shock can easily be calculated ; a typical example is shown in Fig. 21. It is evident that the shock surface will be tangential to the normally incident beam of light both in the two-dimensional region and near the tip, so that a strong image of the two-dimensional shock and a weaker image of the tip shock will be seen on the plate. The theoretical values of the two-dimensional shock angle, calculated from the shock-expansion theory, and of the tip shock angle, obtained on the assumption that the tip pressure coefficient at zero incidence is half the two-dimensional value and that the variation with incidence is according to the linearised theory, are shown in Fig. 20, together with some experimental measurements from the photographs of Fig. 16. In view of the uncertainty of the measurements and of the approximate nature of the theory (*see* the remark at the end of section 2.1) the agreement is quite good at zero and small positive incidences, but not at negative incidences ; this may be due to the large distortion of the tip region in such cases.

The shape of the bow waves seen in the photographs is of less interest in the present connection, since it represents the integrated effect of the purely two-dimensional shock surface from the leading edge. The angles at which the shock detaches are consistent with the theoretical values $\alpha = 5{\cdot}5$, $3{\cdot}2$ and $1{\cdot}0$ deg for the three wings ; thus the thinnest wing at $\alpha = 10$ deg and the two thicker wings at $\alpha = 5$ deg all show detached bow waves. The shock angles at zero incidence are somewhat greater than predicted by theory for $M = 1{\cdot}42$, indicating that the mean Mach number along the leading edge is smaller than the overall mean value ; this was confirmed by the empty-tunnel calibration.

The boundary layer and wake are also in many cases visible in the photographs, but these are again mainly of general interest, and much more detailed information may be obtained from the surface oil patterns.

4.4. *Flow Measurements Off the Wing Surface.*—The results of the measurements of the pressure coefficient C_p and the two components v and w of the perturbation velocity in the vertical plane through the half chord-line ($x = \frac{1}{2}$) are shown in Figs. 6 to 14. They indicate that, in general, the unmodified linearised theory is adequate only for the thinnest wing at very small incidences, outside the immediate neighbourhood of the singularities which exist on the Mach cone from 0 and along the tip chord. The calculations of the strength and position of the conical shock, described in section 2.2.2., are also included in the figures, together with an estimate of the appropriate modifications to the linearised theory ; in most cases the agreement with experiment is considerably improved. In the two-dimensional region inboard of this shock further improvement may be obtained by making use of the Busemann theory to calculate the second approximations to C_p and w/U ; the results are shown in Figs. 12 to 14.

A more detailed discussion of these points is given below :

(*a*) *Along the line* $x = \frac{1}{2}$, $z = 0^*$ ($y > 0$) (Figs. 6 to 8).—At zero incidence the measured pressure coefficients (Fig. 6) are in good agreement with the modified theory for all three wings ; it is difficult to estimate the exact position and strength of the conical shock by means of a static tube, since this causes an apparent smoothing out of the steep pressure rise, but within the limits of the experimental error the predictions of Lighthill's theory[12] are certainly verified. For $\alpha = 2$ deg and 4 deg the predicted constancy of pressure is also verified, but at $\alpha = 6$ deg there is a perceptible increase in the strength of the shock and its displacement from the Mach cone.

The same conclusions are largely true concerning the measurements of v/U (Fig. 7), except that there is an unexpected peak in the experimental curves just inboard of the shock, and variation with incidence is more marked, particularly near the wing tip.

The measurements of w/U (Fig. 8), however, show very poor agreement with theory ; the curves are similar but are displaced laterally so that the measured values are always underestimated. This lateral shift is to be expected near the shock, and for smaller values of y_1 it may perhaps be explained in terms of the displacement due to the separation of the flow at the wing tip ; the peak value of w/U must occur at a positive value of y_1, and again the effect is an outward shift of the origin for y_1.

(*b*) *Along the line* $x = \frac{1}{2}$, $y = 0$ ($z > 0$) (Figs. 9 to 11).—Vertically above the wing tip there are two singularities in the linearised theory ; at the tip ($z_1 = 0$) and at the point $z_1 = 1$ which is common to the two-dimensional region, the tip region and the undisturbed flow. For this reason the agreement between theory and experiment may be expected to be poor, particularly since no second-order corrections are as yet available except as regards the position of the shock, which may be predicted by two-dimensional methods. Nevertheless, at zero incidence the agreement for the thinnest wing is quite good except near the shock ; the variation with thickness is correctly predicted only in the case of v/U.

As the incidence increases the agreement becomes poorer except where local values of the quantity under consideration are very small, in particular the large positive values of w/U which are predicted near the tip are not realised in practice, since the value on the wing surface itself must in fact equal the local inclination of the surface.

The position of the shock is consistent with two-dimensional theory at $\alpha = 0$ and 2 deg except for the thickest wing at $\alpha = 0$, where the relatively small value of z_1 at the shock suggests that this may be beginning to curve from its two-dimensional position into the conical shock from the

*In this section z is measured throughout vertically above the plane of symmetry of the wings, at all incidences ; this fact has been allowed for where necessary in all second-order calculations.

apex. As the incidence increases the strength of the shock decreases, but it does not move towards the plane of the wing as would be expected if the flows over the upper and lower surfaces were independent. Now in fact, for all the wings tested, the shock has detached from the leading edge when the incidence has reached 6 deg, and even before this happens there must be some increase in the curvature of the upper surface shock near the leading edge, with a corresponding upward deflection of the shock from its theoretical position. The strength of the shock is in most cases lower than the theoretical value, which at this point is just half its two-dimensional value.

The experimental values of v/U (Fig. 10) near the tip at the higher incidences are all numerically larger than predicted by theory ; this is clearly consistent with the idea of a tip vortex discussed previously.

(*c*) *Along the line* $x = \frac{1}{2}$, $z = \frac{1}{4}$ (Figs. 12 to 14).—It is convenient to divide the discussion of the results of this horizontal traverse into two parts, outboard ($y > 0$) and inboard ($y < 0$) of the tip respectively. The first of these is analogous to case (*a*) above, and many of the remarks made there are also applicable in the present case. At low incidences ($\alpha = 0$ and 2 deg) reasonably good agreement is obtained for all three quantities between the experimental results and the linearised theory, particularly when the latter is modified according to Lighthill's method to allow for the finite shock strength, though this is overestimated in the case of the two thicker wings.

The variation with incidence, however, differs very considerably from theory, and at $\alpha = 6$ deg the agreement is poor ; in particular, the strength of the shock does not decrease as predicted by theory but remains practically constant, again probably due to the detachment of the shock from the leading edge.

Over the surface of the wing ($y < 0$) the agreement between experiment and the linearised theory depends to some extent on the adequacy of the latter in the two-dimensional region and on the amount of distortion experienced by the tip region, two factors which in the present case are closely connected. Thus at zero incidence, when the second-order correction in the two-dimensional region and the distortion of the tip region are both quite large even for the thinnest wing, the linearised theory gives poor results for C_p and w/U, and the suggested corrections give a considerable improvement, though they cannot at present be extended outside the limit of the two-dimensional region. As the incidence increases the measured values of C_p (Fig. 12) approach more closely to those of the linearised theory, and for $\alpha = 4$ deg and 6 deg the agreement for the thinnest wing is excellent. A similar improvement also takes place in the case of w/U (Fig. 14), but is less marked ; the measured values remain throughout below the theoretical values.

For the sidewash v/U (Fig. 13) the situation is slightly different, since the two-dimensional value is of course exactly zero ; as a result the complete second-order correction can be estimated with some accuracy near the boundary of the tip region, and gives remarkably good results at zero incidence, though the agreement becomes less good as the incidence increases. It is difficult from the experimental measurements to determine the exact position and nature of the boundary of the tip region ; this may be partly due to the rather poor velocity distribution of the empty tunnel in this neighbourhood. However, the reasonably consistent results and satisfactory agreement with theory which are obtained at zero incidence lend some weight to the suggestion that at moderate incidences the simple expansion or shock predicted by theory is replaced in practice by a comparatively diffuse system of weak compression and expansion waves ; compare for example the theoretical and experimental results for v/U at $\alpha = 0$ and 6 deg.

5. *Conclusions.*—The results discussed in the previous section confirm in general the principal that, if detailed information is required concerning the flow over a wing (as opposed to the overall forces acting on it), then the linearised theory is adequate only when the predicted perturbation velocity is small everywhere. Thus, even for the thinnest (4 per cent thick) of the three wings tested, reasonably good experimental agreement with the simple theory is obtained only at zero and very small positive incidences at points not too near the singularities

which exist at the wing tip and on the Mach cone from the apex. The tip singularity at incidence is of order $r^{-1/2}$, while at zero incidence it is merely logarithmic, and it is probably for this reason that in general the effect of increasing incidence is estimated with less accuracy than the flow at zero incidence.

Certain modifications to the linearised theory in the neighbourhood of the conical singularity (based on Lighthill's method[12]), which predict in particular its strength and position, provide a definite improvement at low incidences but are again less successful when the incidence is appreciable. No complete second-order theory is yet available, but the pressure on the upper surface of the wings at positive incidences may be estimated with some success by a simple extention of the shock-expansion method for two-dimensional flow. Good agreement with experiment is obtained in this way at incidences up to about 10 deg in regions which are not too close to the wing tip and are not affected by trailing-edge separation. At zero and small negative incidences further improvement may be obtained by using a modification suggested by Czarnecki and Mueller[5] to take into account the distortion of the tip region, which at these incidences may be considerable ; at positive incidences, however, the corresponding modification seems less successful.

Surface oil patterns (Fig. 17) confirm the existence at high incidences of vortices lying in a streamwise direction above the upper surface at the wing tips, as in subsonic flow ; these tip vortices lead to a local increase in suction which is evident in the surface pressure measurements in this region. The degree of separation of the boundary layer near the trailing edge is consistent with previous two-dimensional work on the subject[21, 22, 23] ; the separation always starts in the two-dimensional region and spreads outwards towards the tip, but does not reach it within the incidence range of the present tests.

The reflection plate was used successfully as a screen on which to obtain direct shadowgraphs. The most interesting results obtained in this way concern the nature of the trailing-edge shock ; this is apparent in the photographs (Fig. 16) as an apparent bifurcation of the shock, which is shown to be consistent with theoretical considerations on the shape of the shock surface.

The comparatively low supersonic Mach number of the present tests leads to the detachment of the leading-edge shock over a large part of the range of incidence, particularly for the thicker wings. For this reason it would be interesting to investigate the effect of increasing the Mach number ; this might lead to better agreement with theory in regions near the leading edge. Further work should also include flow measurements downstream of the trailing edge, which have not been attempted with the present apparatus, due to the poor quality in this region of the flow produced by the reflection plate.

Acknowledgements.—Particular acknowledgements are due to Mr. C. J. Berry, who was responsible for much of the experimental work described in this paper, and to Miss B. M. Davis and Mr. G. F. Lee for their assistance in the computations and experiments.

LIST OF PRINCIPAL SYMBOLS

x, y, z	Non-dimensional co-ordinates
U	Free-stream velocity
u, v, w	Components of perturbation velocity
c	Wing chord
τ	Thickness ratio
ϕ	Velocity potential

LIST OF PRINCIPAL SYMBOLS—*continued*

M Free-stream Mach number

$B = \sqrt{(M^2 - 1)}$

ρ Density

p Static pressure

} The suffix $_1$ denotes value in the free stream

α Wing incidence

ε Downwash angle

$y_1 = By/x$

$z_1 = Bz/x$

} Conical co-ordinates

$r = B\sqrt{(y^2 + z^2)}/x = \sqrt{(y_1^2 + z_1^2)}$

$\theta = \tan^{-1}(z/y)$

$\psi = \tan^{-1}(-y_1)$

$C_p = (p - p_1)/(\frac{1}{2}\rho_1 U^2)$. Pressure coefficient

ω Inclination of shock to the free-stream direction

REFERENCES

No.	*Author*	*Title, etc.*
1	M. J. Lighthill	The supersonic theory of wings of finite span. R. & M. 2001. October, 1944.
2	E. A. Bonney	Aerodynamic characteristics of rectangular wings at supersonic speeds. *J. Ae. Sci.* 14. p. 110. 1947.
3	C. Picard and J. P. Chevalier	Mesures de pressions et d'efforts sur une demi-aile rectangulaire en supersonique. *La Recherche Aéronautique* No. 26. p. 3. 1952.
4	W. G. Vincenti	Comparison between theory and experiment for wings at supersonic speeds. N.A.C.A. Tech. Note 2100. 1950.
5	K. R. Czarnecki and J. N. Mueller ..	An approximate method of calculating pressures in the tip region of a rectangular wing at supersonic speeds. N.A.C.A. Tech. Note 2211. 1950.
6	G. N. Ward	*Linearised theory of high speed flow.* Cambridge University Press.
7	S. Goldstein and G. N. Ward	The linearised theory of conical fields in supersonic flow. *Aero. Quart.* 2. 39. 1950.
8	P. A. Lagerstrom and M. E. Graham ..	Downwash and sidewash induced by three-dimensional lifting wings in supersonic flow. Douglas Aircraft Co. Report SM–13007. 1947.
9	M. J. Lighthill	Two-dimensional supersonic aerofoil theory. R. & M. 1929. January, 1944.
10	M. J. Lighthill	The conditions behind the trailing edge of the supersonic aerofoil. R. & M. 1930. January, 1944.
11	M. J. Lighthill	A technique for rendering approximate solutions to physical problems uniformly valid. *Phil. Mag.* (7). 40. 1179. 1949.

REFERENCES—*continued*

No.	*Author.*	*Title, etc.*
12	M. J. Lighthill	The shock strength in supersonic conical fields. *Phil Mag.* (7). 40. 1202. 1949.
13	D. W. Holder	The 18 in. × 14 in. High-Speed Wind Tunnel at the N.P.L. (Unpublished.)
14	A. O. Ormerod	An investigation of the disturbances caused by a reflection plate in the working-section of a supersonic wind tunnel. R. & M. 2799. November, 1950.
15	D. E. Coletti	Investigation of the effects of model scale and stream Reynolds number on the aerodynamic characteristics of two rectangular wings at supersonic speeds. N.A.C.A. Research Memo. L55D29. 1955.
16	H. K. Cheng	Aerodynamics of a rectangular plate with vortex separation in supersonic flow. *J. Ae. Sci.* 22. 217. 1955.
17	R. H. Edwards	Leading-edge separation from slender delta wings. *J. Ae. Sci.* 21 134. 1954.
18	Mac C. Adams	Leading-edge separation from delta wings at supersonic speeds. Readers' Forum. *J. Ae. Sci.* 20. 430. 1953.
19	C. E. Brown and W. H. Michael ..	On slender delta wings with leading edge separation. N.A.C.A. Tech. Note 3430. 1955.
20	D. Küchemann	A non-linear lifting-surface theory for wings of small aspect ratio with edge separation. R.A.E. Report Aero. 2540. A.R.C. 17,769. April, 1955.
21	G. E. Gadd, D. W. Holder and J. D. Regan	An experimental investigation of the interaction between shock waves and boundary layers. *Proc. Roy. Soc.* (A). 226. 227. 1954.
22	G. E. Gadd and D. W. Holder ..	Boundary-layer separation in two-dimensional supersonic flow C.P.270. March, 1955.
23	B. D. Henshall and R. F. Cash ..	The interaction between shock waves and boundary layers at the trailing edge of a double-wedge aerofoil at supersonic speed. R. & M. 3004. March, 1955.

APPENDIX

The Flow Field Due to a Rectangular Biconvex Wing (Linearised Theory)

(*a*) *Zero incidence.*—The perturbation velocity due to a distribution of supersonic sources of strength $2\tau(1 - 2x)$, over the semi-infinite strip $0 \leqslant x \leqslant 1$, $y < 0$, has to be calculated. This may of course be done by first finding the velocity potential (*e.g.*, by direct integration) and then differentiating ; but it is instructive to build up the velocity field from that of a rectangular wedge, which may easily be determined by the method of Goldstein and Ward[6,7] for conical flow.

Consider first a wedge of semi-angle δ, at zero incidence, occupying the quadrant $x > 0$, $y < 0$. Next use the conical co-ordinates $y_1 = By/x = r\cos\theta$, $z_1 = Bz/x = r\sin\theta$, and make the standard transformation to the complex t plane, defined by

$$t = r/(\cos\theta - i\sqrt{(1 - r^2)}\sin\theta) \quad (r \leqslant 1) \qquad (A.1)$$
$$= \operatorname{sech}(s + i\theta),$$

where $$s = -\cosh^{-1}\frac{1}{r}.$$

It is then well known that the general conical velocity field satisfying the linearised equations of motion may be written $u = \mathscr{R}G_1(t)$, $v = \mathscr{R}G_2(t)$, and $w = \mathscr{R}G_3(t)$, where G_1, G_2 and G_3 are analytic functions of t satisfying the relations

$$G_1'(t) : G_2'(t) : G_3'(t) = \frac{it}{B} : -i : \sqrt{(1-t^2)} \; . \qquad \text{(A.2)}$$

The boundary conditions to be satisfied in the t plane are :

On the real axis : $\mathscr{R}(t) > 0$, $w = 0$.

On the real axis : $\mathscr{R}(t) < 0$, $w = \pm U\delta$.

These are clearly satisfied by

$$G_3(t) = -i\frac{U\delta}{\pi}\log t \, , \qquad \text{(A.3)}$$

whence
$$w = \frac{U\delta}{\pi}\operatorname{Am} t$$

$$= \frac{U\delta}{\pi}\tan^{-1}\{\sqrt{(1-r^2)}\tan\theta\} \text{ from (A.1)}$$

$$= \frac{U\delta}{\pi}\operatorname{sgn} z \cos^{-1}\frac{y_1}{r\sqrt{(1-z_1^2)}} \; . \qquad \text{(A.4)}$$

From (A.2), it is easily found that

$$G_1 = -\frac{U\delta}{\pi B}\cos^{-1} t \qquad \text{(A.5)}$$

and
$$G_2 = -\frac{U\delta}{\pi}\cosh^{-1}\frac{1}{t} \; . \qquad \text{(A.6)}$$

Thus
$$u = -\frac{U\delta}{\pi B}\operatorname{Am}\{t + i\sqrt{(1-t^2)}\} \, ,$$

and since

$$\sqrt{(1-t^2)} = \frac{\sqrt{(1-r^2)} - ir^2\sin\theta\cos\theta}{1 - r^2\sin^2\theta} \, ,$$

it follows that
$$u = -\frac{U\delta}{\pi B}\cos^{-1}\frac{y_1}{\sqrt{(1-z_1^2)}} \; . \qquad \text{(A.7)}$$

Since $\cosh^{-1}\dfrac{1}{t} = s + i\theta$, it also follows that

$$v = \frac{\delta U}{\pi}\cosh^{-1}\frac{1}{r} \; . \qquad \text{(A.8)}$$

Transformation back to cartesian co-ordinates yields

$$\frac{u}{U} = -\frac{\delta}{\pi B}\cos^{-1}\frac{By}{\sqrt{(x^2 - B^2z^2}}, \qquad \text{(A.9)}$$

$$\frac{v}{U} = \frac{\delta}{\pi}\cosh^{-1} x/(B\tilde{\omega}), \qquad \text{(A.10)}$$

and

$$\frac{w}{U} = \frac{\delta}{\pi}\operatorname{sgn} z \cos^{-1} xy/\{\tilde{\omega}\sqrt{(x^2 - B^2z^2)}\}, \qquad \text{(A.11)}$$

where $\tilde{\omega} = \sqrt{(y^2 + z^2)}$.

Now the actual wing may be thought of as made up of a wedge of semi-angle $\delta_0 = 2\tau$ with leading edge along $x = 0$, together with a distribution of infinitesimal wedges, each of semi-angle $-4\tau\,\delta\xi$ with leading edges along $x = \xi$ at intervals $\delta\xi$ in the streamwise direction. Since the point (x, y, z) $(z > 0)$ is inside the Mach cones from the apex of those wedges for which $0 \leqslant \xi \leqslant x - B\tilde{\omega}$, and inside the two-dimensional region of wedges with $x - B\tilde{\omega} \leqslant \xi \leqslant x - Bz$ (for $y < 0$), it follows that, for $z > 0$:

$$\frac{u}{U} = -\frac{2\tau}{\pi B}\cos^{-1}\frac{y_1}{\sqrt{(1 - z_1^2)}} + \frac{4\tau}{\pi B} I_1, \qquad \text{(A.12)}$$

$$\frac{v}{U} = \frac{2\tau}{\pi}\cosh^{-1}\frac{1}{r} - \frac{4\tau}{\pi} I_2, \qquad \text{(A.13)}$$

and

$$\frac{w}{U} = \frac{2\tau}{\pi}\cos^{-1}\frac{xy}{\tilde{\omega}\sqrt{(x^2 - B^2z^2)}} - \frac{4\tau}{\pi} I_3, \qquad \text{(A.14)}$$

where

$$I_1 = \int_{B\tilde{\omega}}^{x} \cos^{-1}\frac{By}{\sqrt{(\zeta^2 - B^2z^2)}}\,d\zeta + \pi B(\tilde{\omega} - z)H(-y),$$

$$I_2 = \int_{B\tilde{\omega}}^{x} \cosh^{-1}\frac{\zeta}{B\tilde{\omega}}\,d\zeta,$$

and

$$I_3 = \int_{B\tilde{\omega}}^{x} \cos^{-1}\frac{y\zeta}{\tilde{\omega}\sqrt{(\zeta^2 - B^2z^2)}}\,d\zeta + \pi(\tilde{\omega} - z)H(-y).$$

These integrals can be evaluated by integration by parts ; in the case of I_1 and I_3 the further substitutions

$$\frac{\zeta}{\sqrt{(\zeta^2 - B^2\tilde{\omega}^2)}} = \xi \text{ (for } I_1)$$

and

$$\frac{1}{\sqrt{(\zeta^2 - B^2\tilde{\omega}^2)}} = \eta \text{ (for } I_3) \text{ are necessary.}$$

Then it may be shown that

$$I_2 = x\cosh^{-1}\frac{1}{r} - x\sqrt{(1 - r^2)}.$$

When y is positive, it is found that

$$I_1 = x\cos^{-1}\frac{y_1}{\sqrt{(1-z_1^2)}} - By\cosh^{-1}\frac{1}{r} - Bz\cos^{-1}\frac{y_1}{r\sqrt{(1-z_1^2)}}.$$

When y is negative

$$I_1 = \int_{B\bar{\omega}}^{x}\left\{\pi - \cos^{-1}\frac{B|y|}{\sqrt{(\zeta^2 - B^2z^2)}}\right\}d\zeta + \pi B(\bar{\omega} - z)$$

$$= \pi(x - Bz) - x\cos^{-1}\frac{|y_1|}{\sqrt{(1-z_1^2)}} + B|y|\cosh^{-1}\frac{1}{r} + Bz\cos^{-1}\frac{|y_1|}{r\sqrt{(1-z_1^2)}}$$

$$= x\cos^{-1}\frac{y_1}{\sqrt{(1-z_1^2)}} - By\cosh^{-1}\frac{1}{r} - Bz\cos^{-1}\frac{y_1}{r\sqrt{(1-z_1^2)}},$$

as for positive y.

Similarly, for positive and negative y :

$$I_3 = x\cos^{-1}\frac{y_1}{r\sqrt{(1-z_1^2)}} - Bz\cos^{-1}\frac{y_1}{\sqrt{(1-z_1^2)}}.$$

Finally, considerations of symmetry lead to the result that, for all z :

$$\frac{u}{U} = -\frac{2\tau}{\pi}\left[\frac{1}{B}(1-2x)\cos^{-1}\frac{y_1}{\sqrt{(1-z_1^2)}} + 2|z|\cos^{-1}\frac{y_1}{r\sqrt{(1-z_1^2)}} + 2y\cosh^{-1}\frac{1}{r}\right] \quad \text{(A.15)}$$

$$\frac{v}{U} = \frac{2\tau}{\pi}\left[(1-2x)\cosh^{-1}\frac{1}{r} + 2x\sqrt{(1-r^2)}\right] \quad \text{(A.16)}$$

and

$$\frac{w}{U} = \frac{2\tau}{\pi}\operatorname{sgn} z\left[(1-2x)\cos^{-1}\frac{y_1}{r\sqrt{(1-z_1^2)}} + 2B|z|\cos^{-1}\frac{y_1}{\sqrt{(1-z_1^2)}}\right]. \quad \text{(A.17)}$$

(*b*) *Flow due to incidence.*—The solution for a rectangular plate at incidence α is well known ; it is given, when $z > 0$, by

$$\frac{\pi G_1(t)}{2U\alpha} = -\frac{i}{B}\tanh^{-1}\sqrt{\left(\frac{t}{1+t}\right)} = -\frac{2i}{\pi B}\sinh^{-1}\sqrt{t}, \quad \text{(A.18)}$$

$$\frac{\pi G_2(t)}{2U\alpha} = -i\sqrt{\left(\frac{1+t}{t}\right)}, \quad \text{(A.19)}$$

and

$$\frac{\pi G_3(t)}{2U\alpha} = \sqrt{\left(\frac{1-t}{t}\right)} - \tan^{-1}\sqrt{\left(\frac{1-t}{t}\right)}. \quad \text{(A.20)}$$

[These equations may be obtained either directly, by using the boundary conditions

$R(G_3') = 0$ for $t < 0$

and $I(G_3') = 0$ for $t > 0$,

or from equations (112) to (114) of Goldstein and Ward's paper[7], putting $t_0 = \infty$, $t_2 = 0$].

By making use of the relation

$$\left(\frac{1 \pm t}{t}\right)^{1/2} = r^{-1/2}[(1 \pm r)^{1/2} \cos \tfrac{1}{2}\theta - i(1 \mp r)^{1/2} \sin \tfrac{1}{2}\theta],$$

which may be deduced from the definition of t (A.1), the equations valid for $z_1 > 0$ can be obtained, namely

$$\frac{u}{U} = \frac{\alpha}{\pi B} \cos^{-1} \frac{1 - r + y_1}{\sqrt{(1 - z_1^2)}}, \qquad \text{(A.21)}$$

$$\frac{v}{U} = -\frac{2\alpha}{\pi} \sqrt{\left(\frac{1 - r}{r}\right)} \sin \tfrac{1}{2}\theta, \qquad \text{(A.22)}$$

and

$$\frac{w}{U} = \frac{2\alpha}{\pi} \left[\sqrt{\left(\frac{1 - r}{r}\right)} \cos \tfrac{1}{2}\theta + \tfrac{1}{2} \cos^{-1} \frac{1 - r - y_1}{\sqrt{(1 - z_1^2)}} - \frac{\pi}{2} \right]. \qquad \text{(A.23)}$$

These results can easily be extended to cover negative values of z by considerations of anti-symmetry ; and by combining them with equations (A.15) to (A.17), equations (4) to (6) of section 2.1 may be derived.

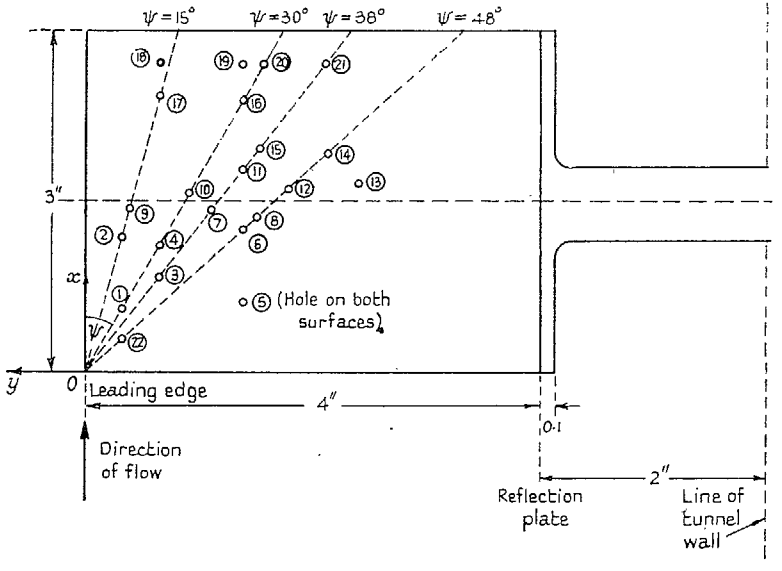

FIG. 1. Plan of model, showing position of pressure holes.

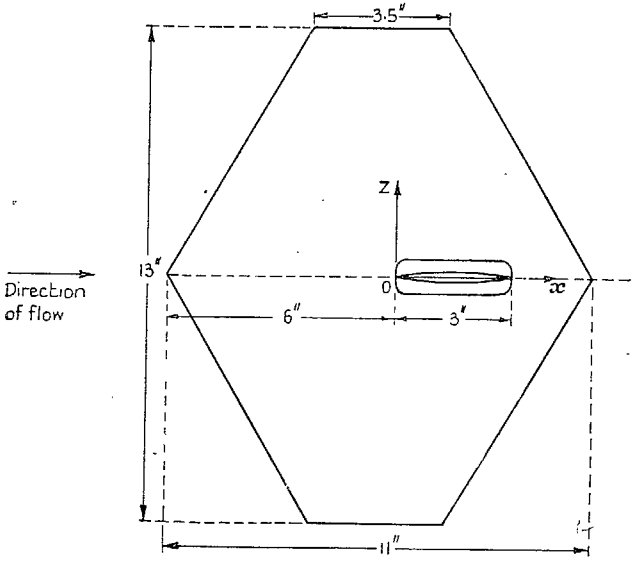

FIG. 2. Position of model in reflection plate.

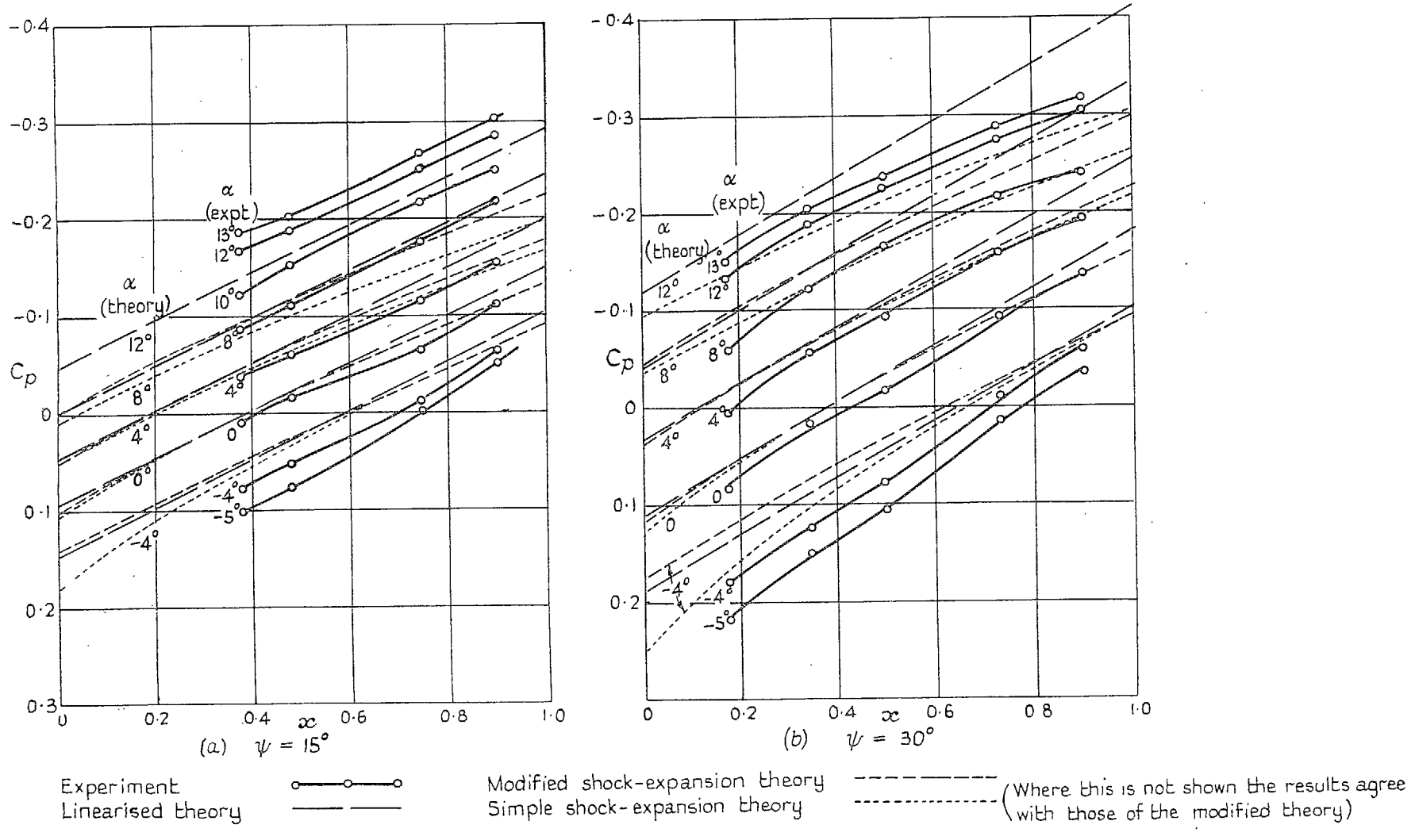

FIGS. 3a and 3b. Pressure distribution on the wing.—$\tau = 0{\cdot}04$.

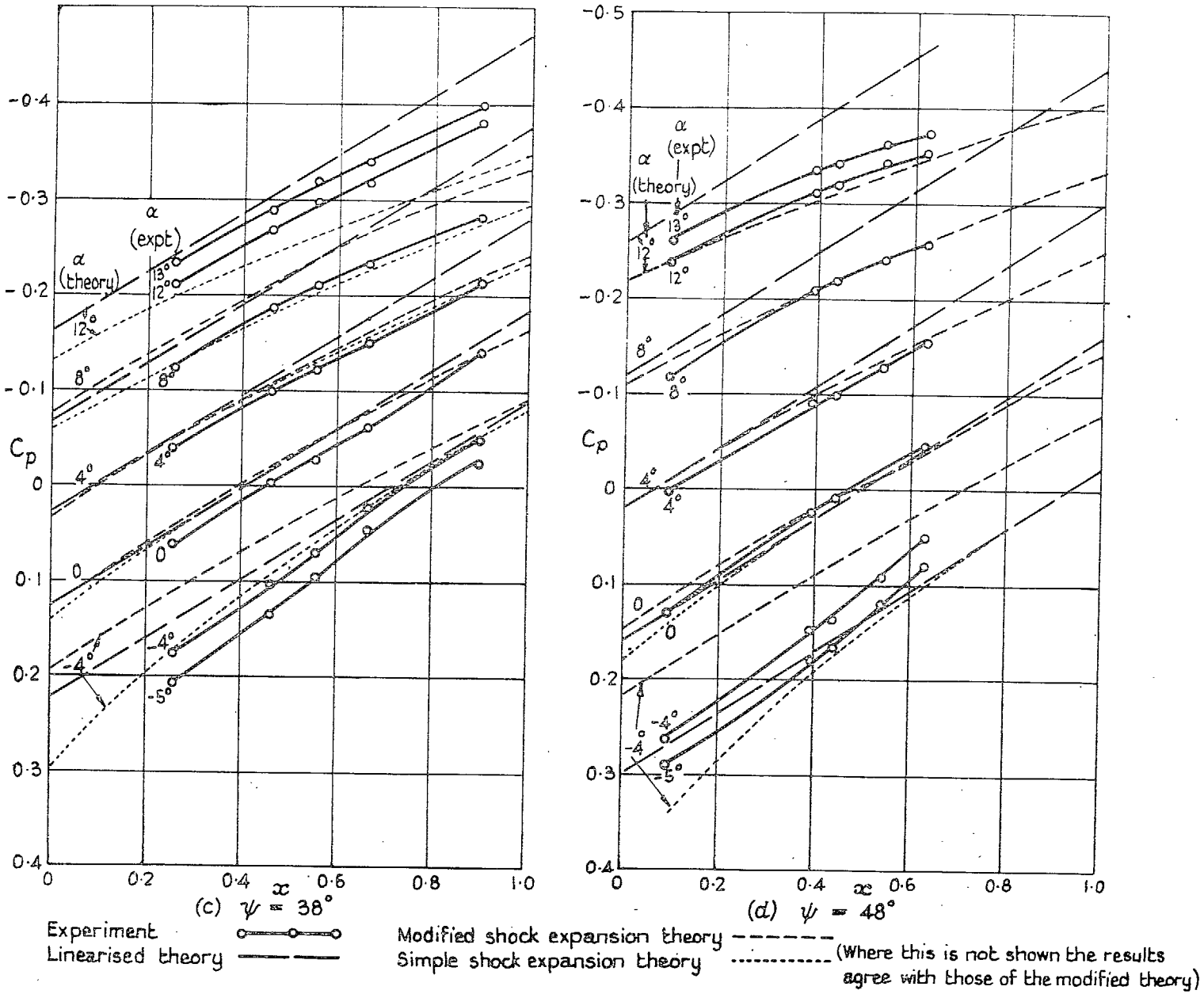

FIGS. 3c and 3d. Pressure distribution on the wing.—$\tau = 0{\cdot}04$.

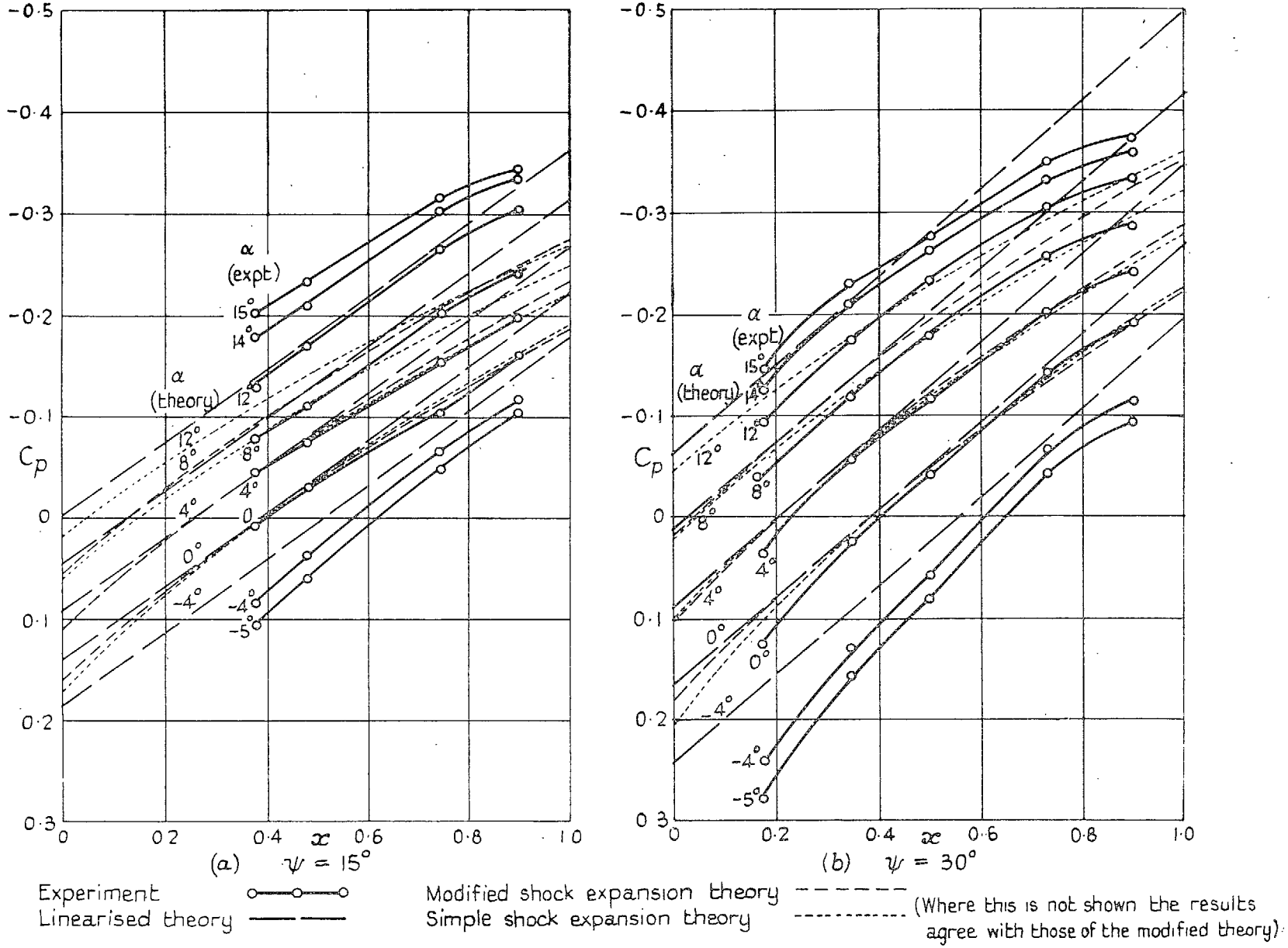

FIGS. 4a and 4b. Pressure distribution on the wing.—$\tau = 0{\cdot}06$.

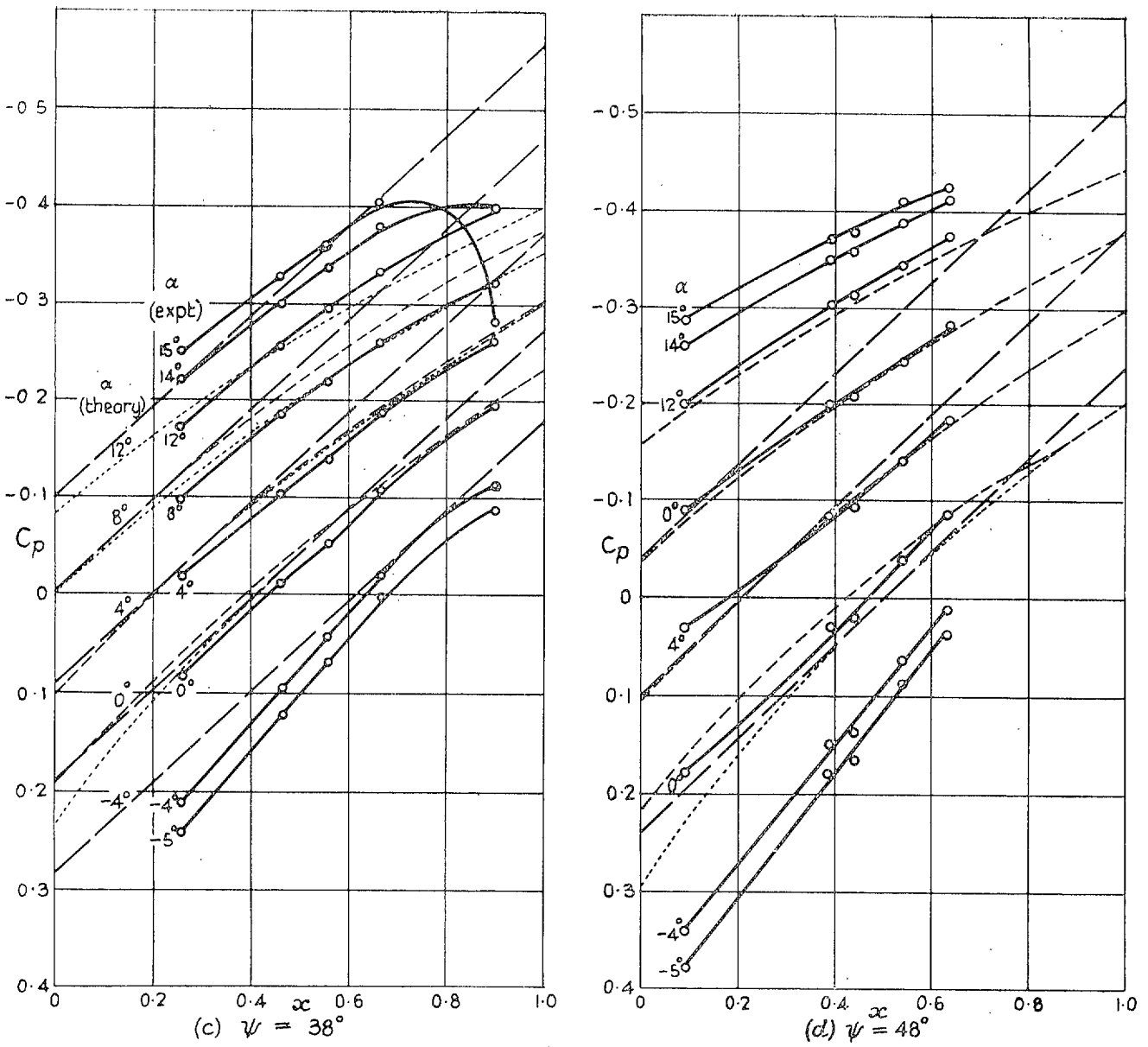

FIGS. 4c and 4d. Pressure distribution on the wing.—$\tau = 0{\cdot}06$.

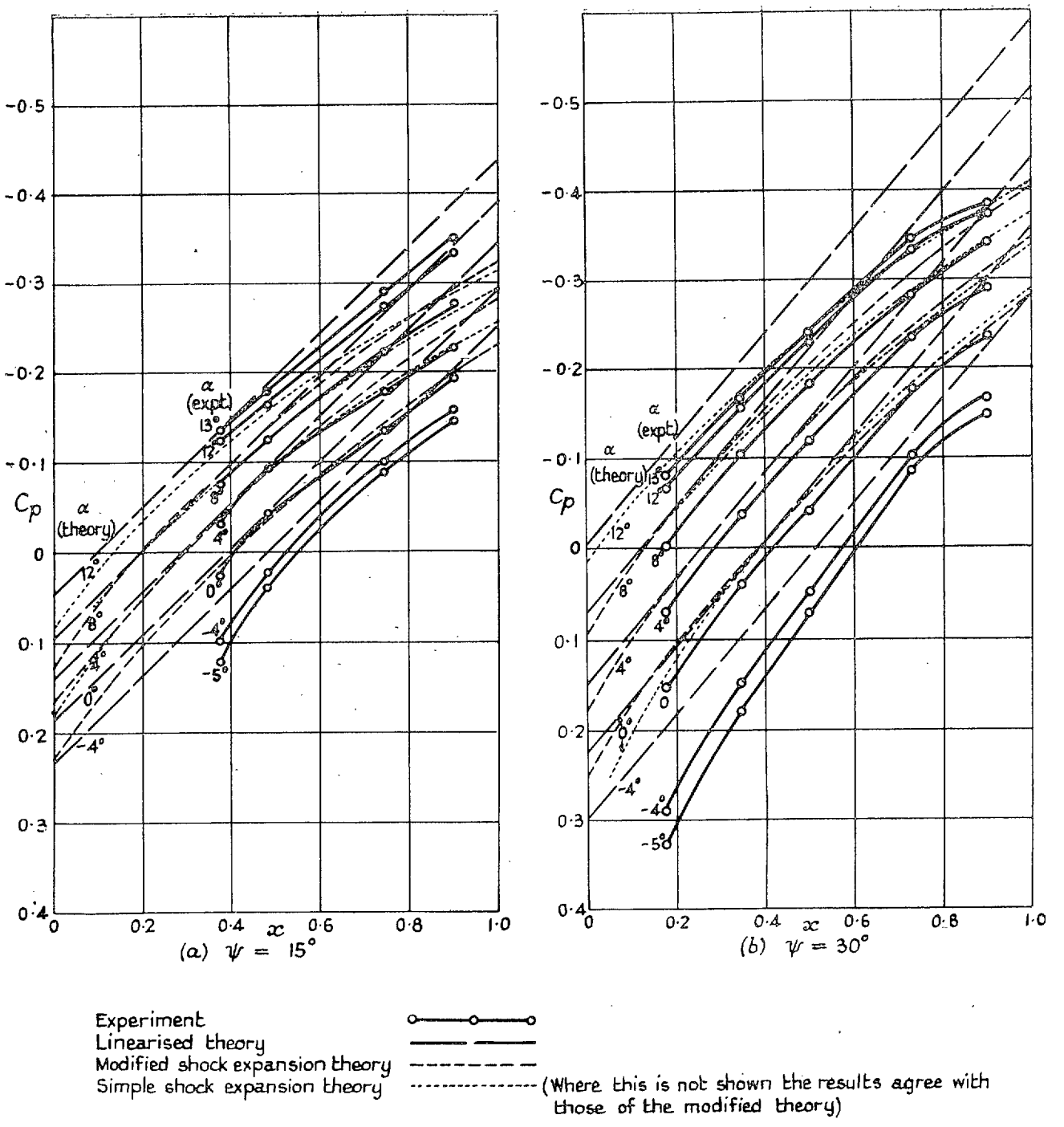

FIGS. 5a and 5b. Pressure distribution on the wing.—$\tau = 0{\cdot}08$.

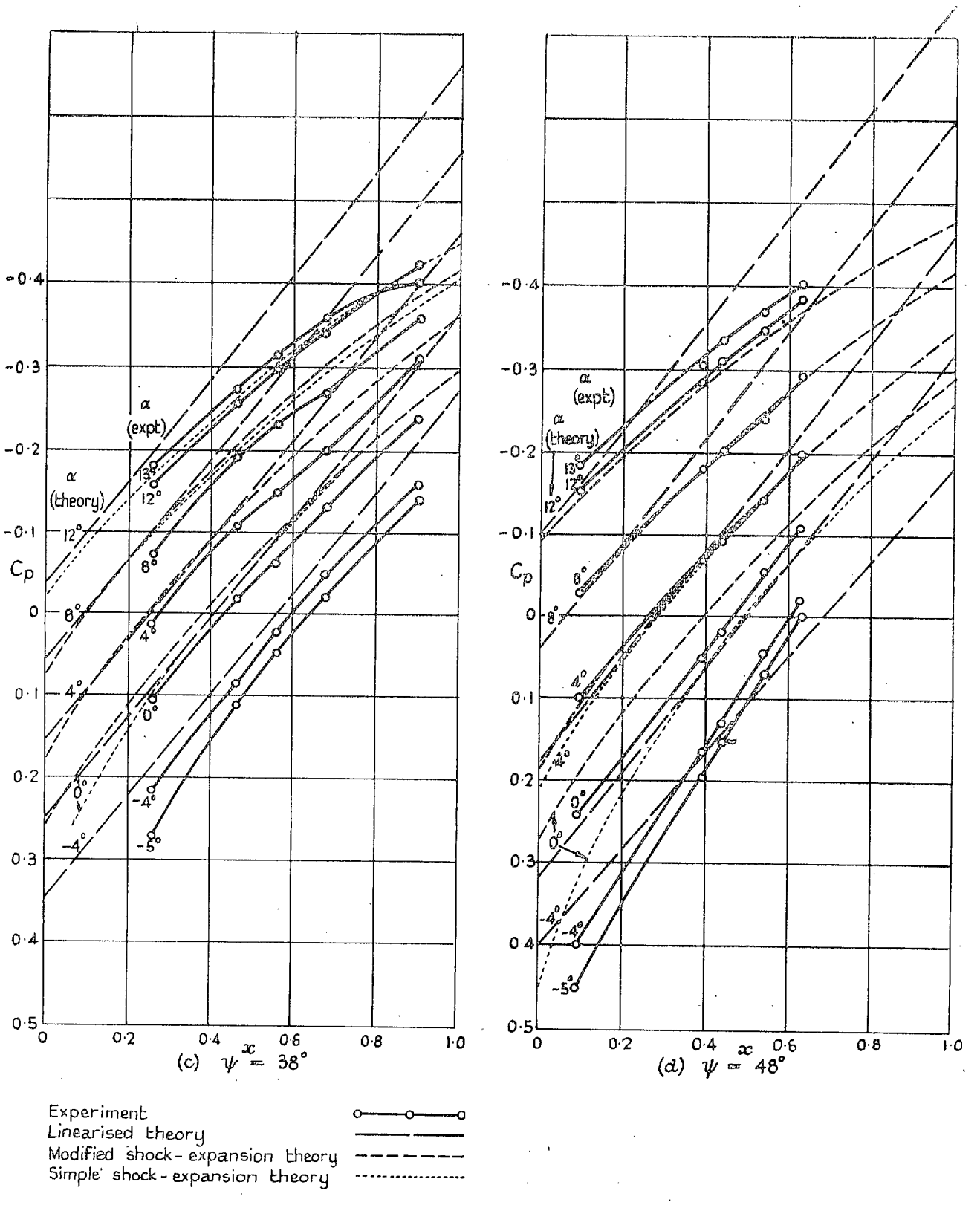

FIGS. 5c and 5d. Pressure distribution on the wing.—$\tau = 0{\cdot}08$.

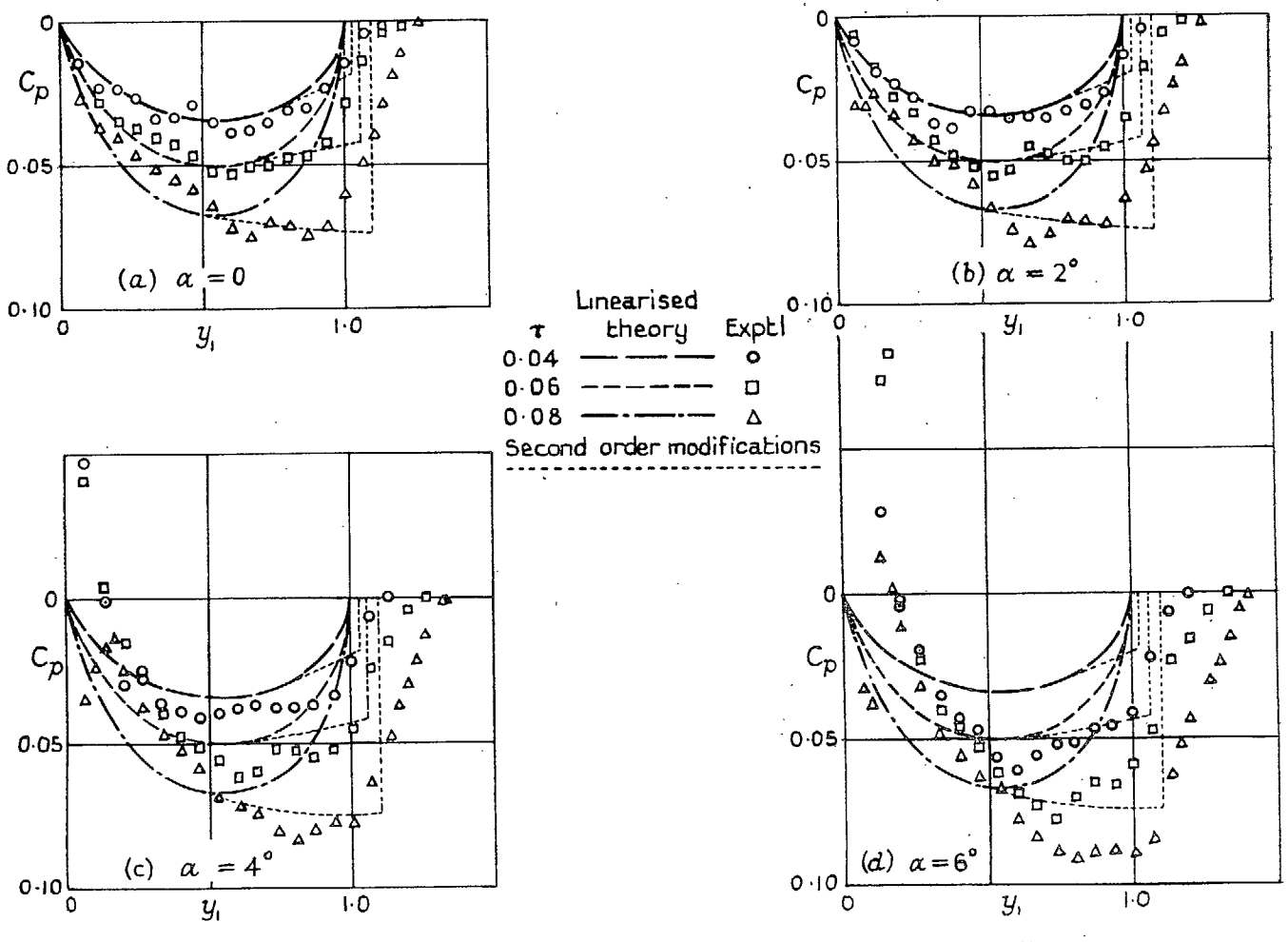

FIG. 6. Pressure coefficients along model centre-line ($x = 0{\cdot}5$, $z = 0$).

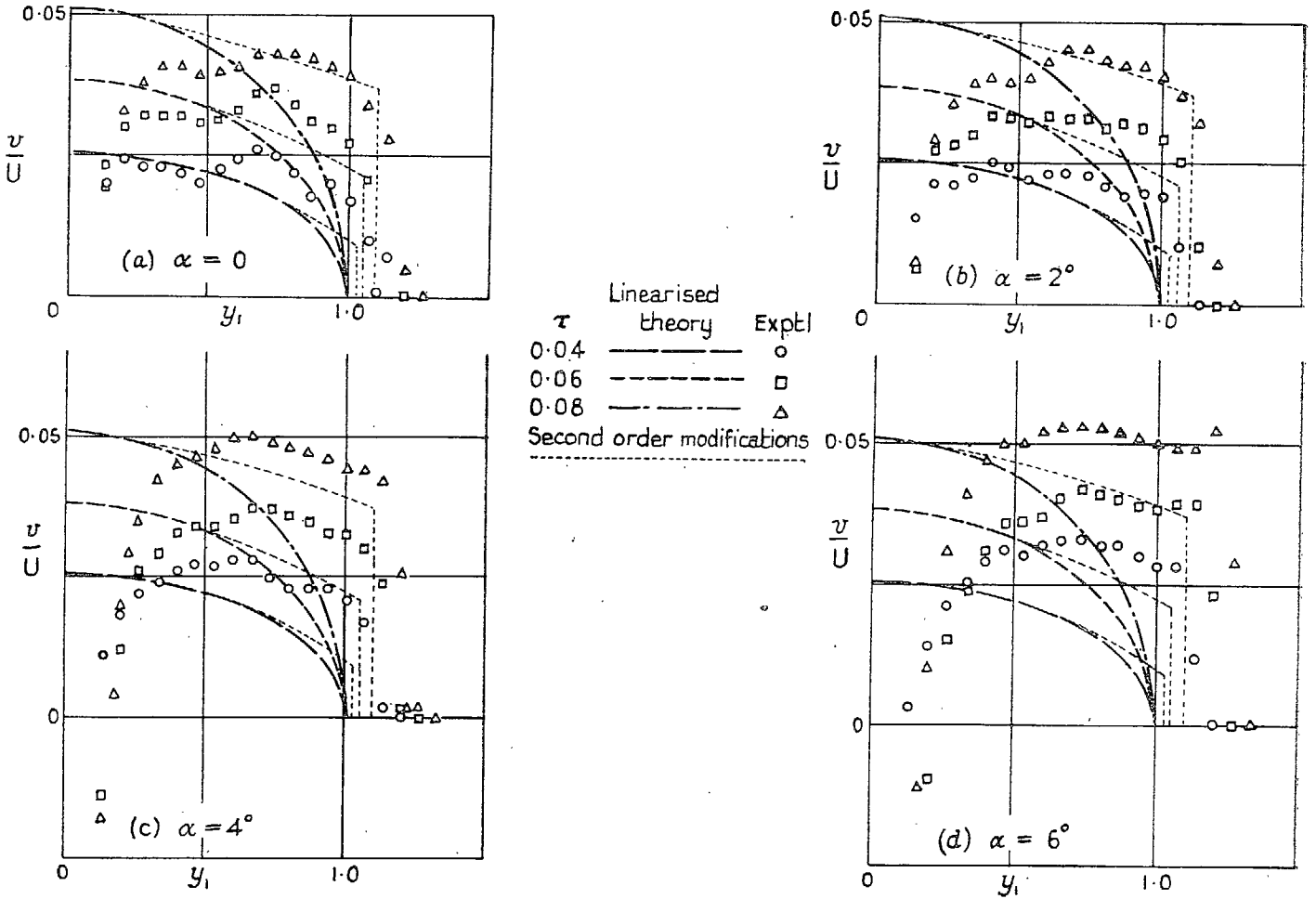

FIG. 7. Transverse component of velocity along model centre-line ($x = 0{\cdot}5$, $z = 0$).

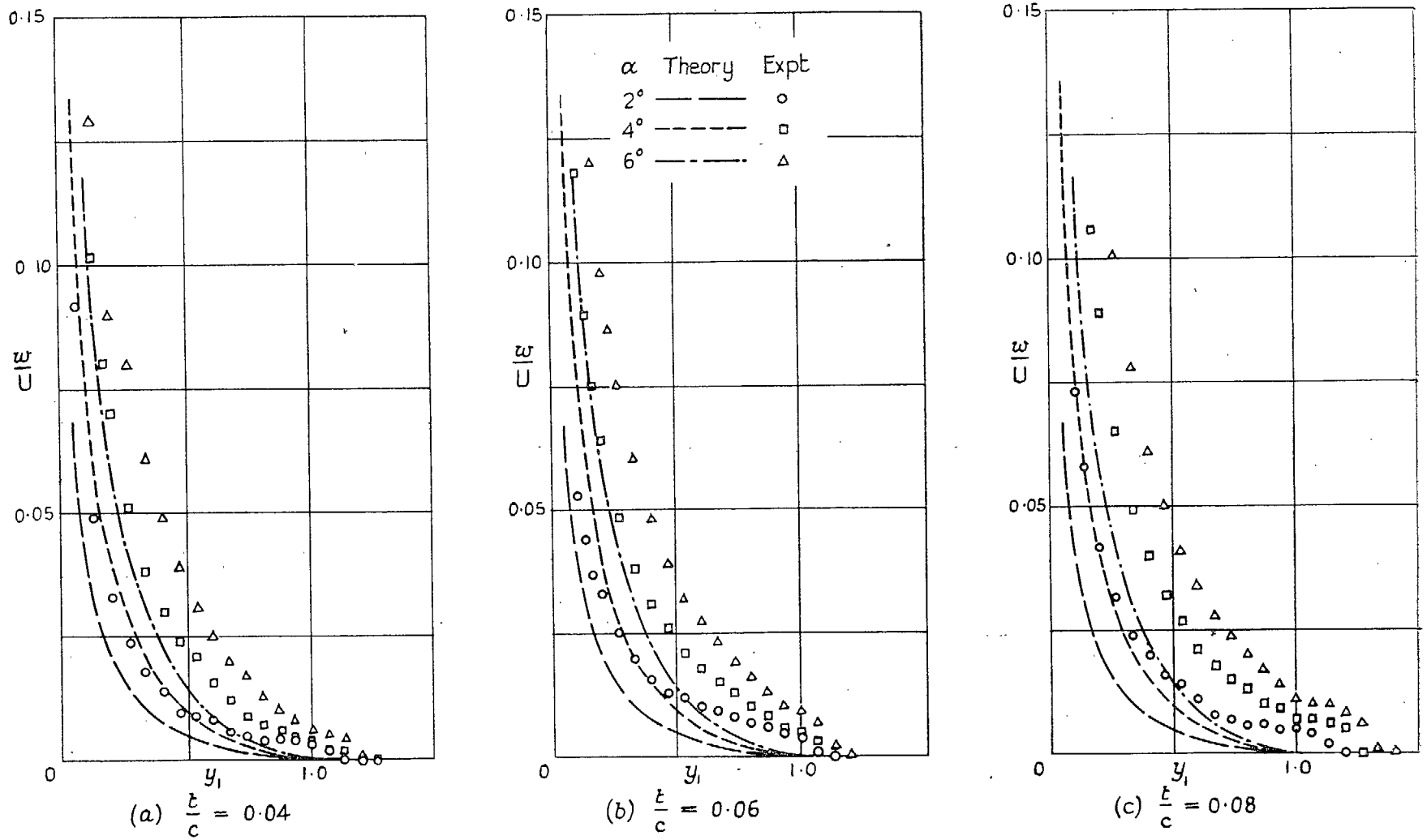

FIG. 8a to 8c. Vertical component of velocity along model centre-line ($x = 0{\cdot}5, z = 0$).

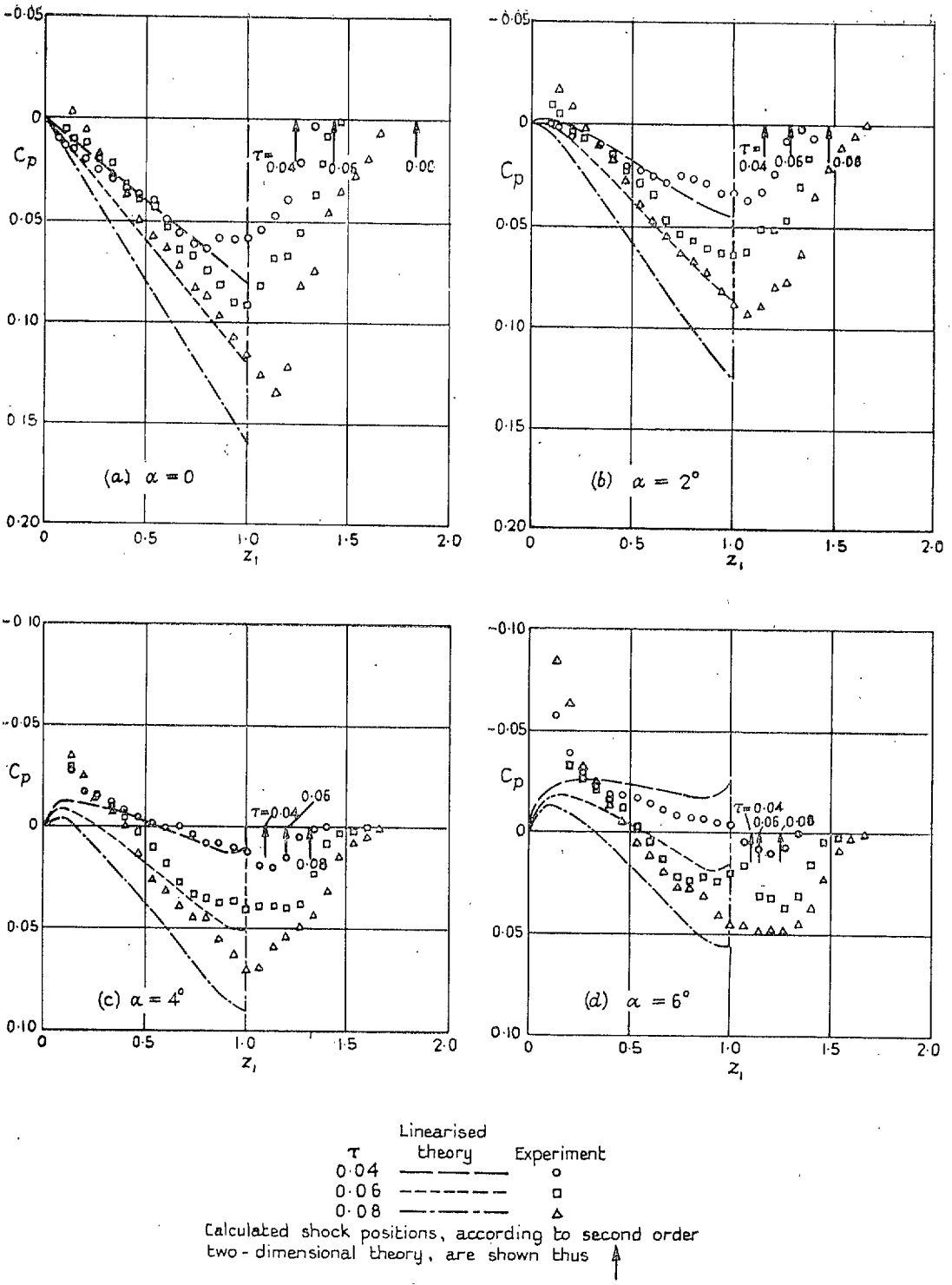

FIG. 9. Pressure coefficients vertically above centre of wing tip ($x = 0{\cdot}5, y = 0$).

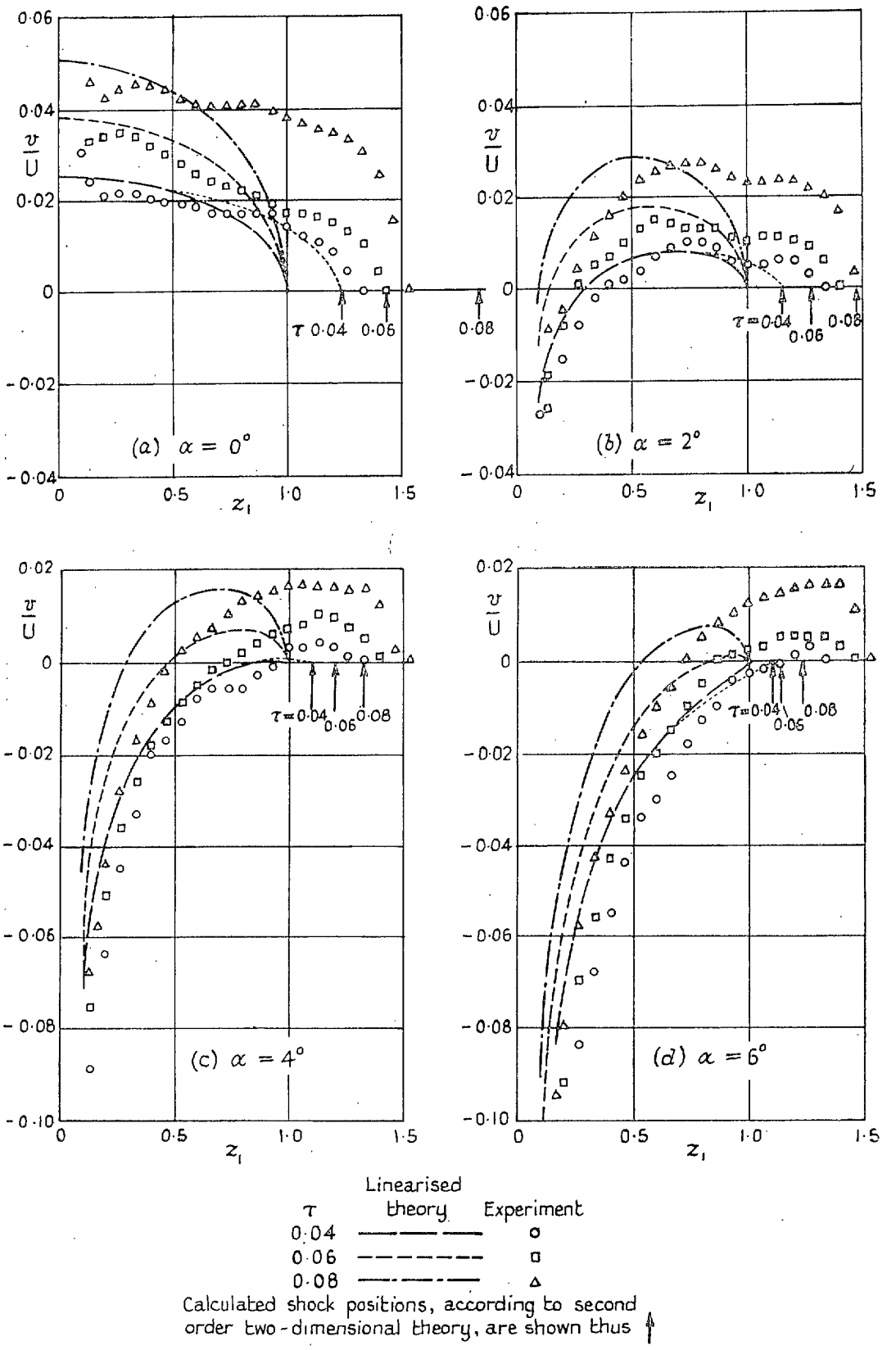

FIG. 10. Transverse component of velocity vertically above centre of wing tip ($x = 0{\cdot}5, y = 0$).

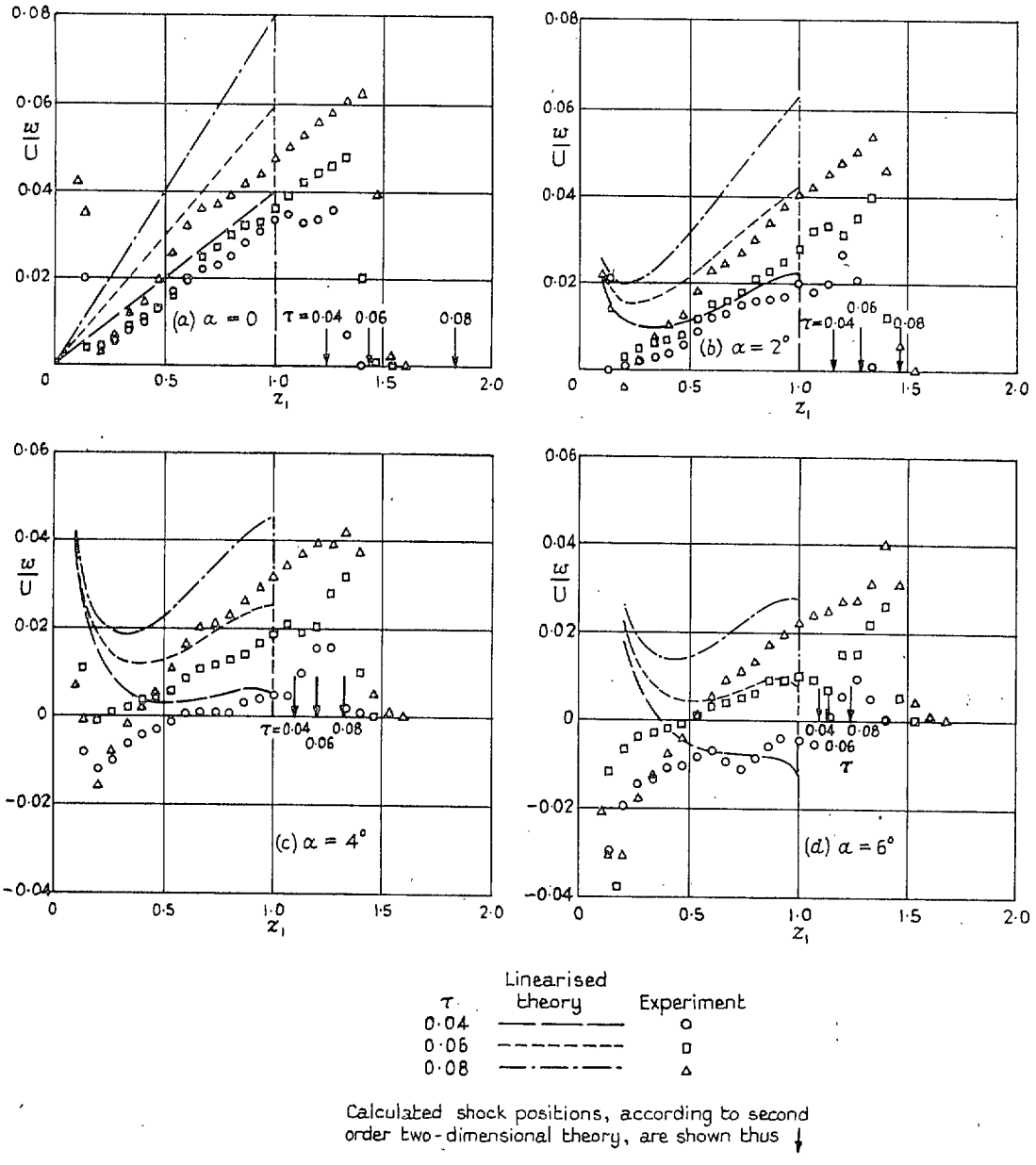

FIG. 11. Vertical component of velocity vertically above centre of wing tip ($x = 0{\cdot}5, y = 0$).

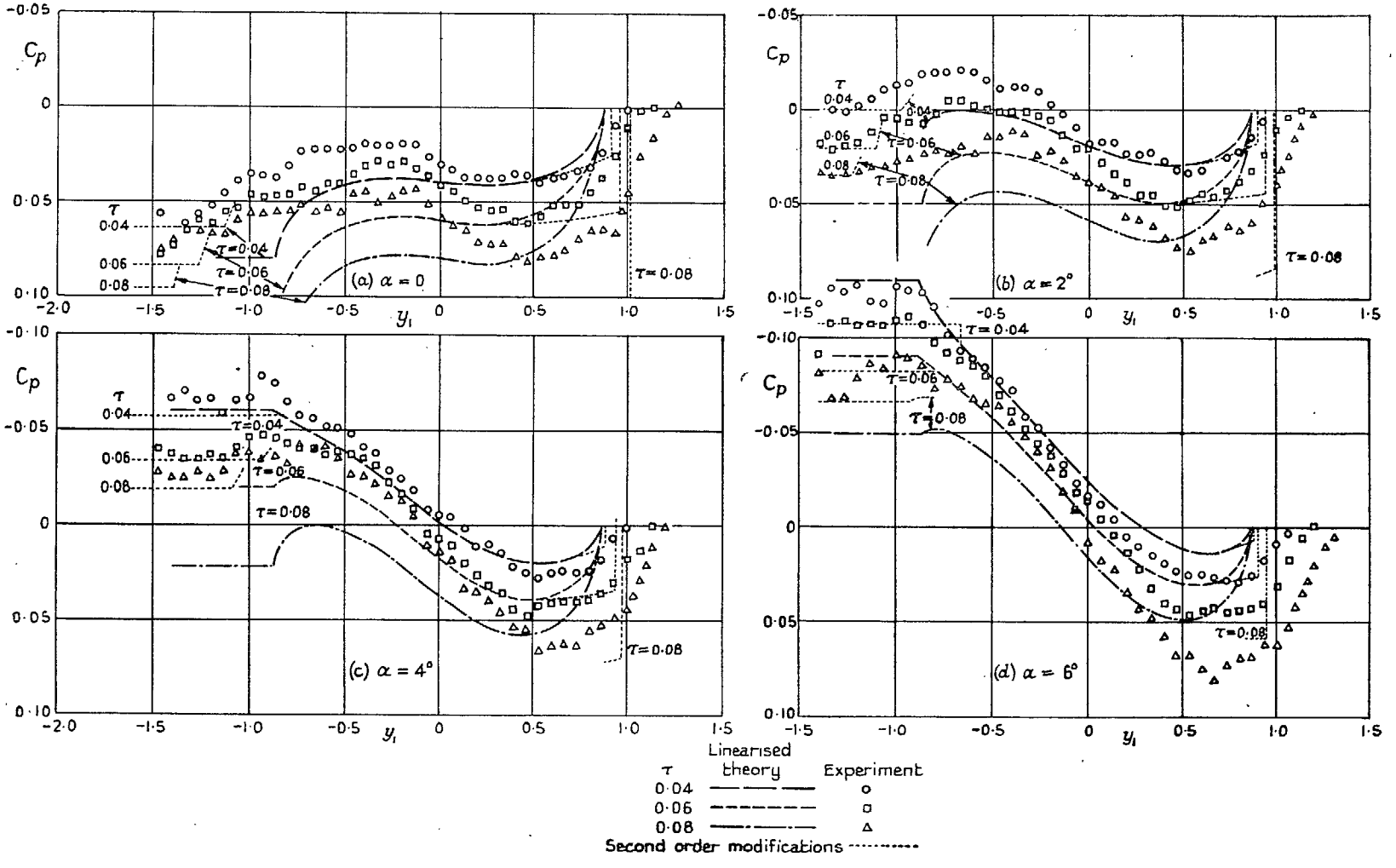

FIG. 12. Pressure coefficients along the line $x = 0{\cdot}5$, $z = 0{\cdot}25$.

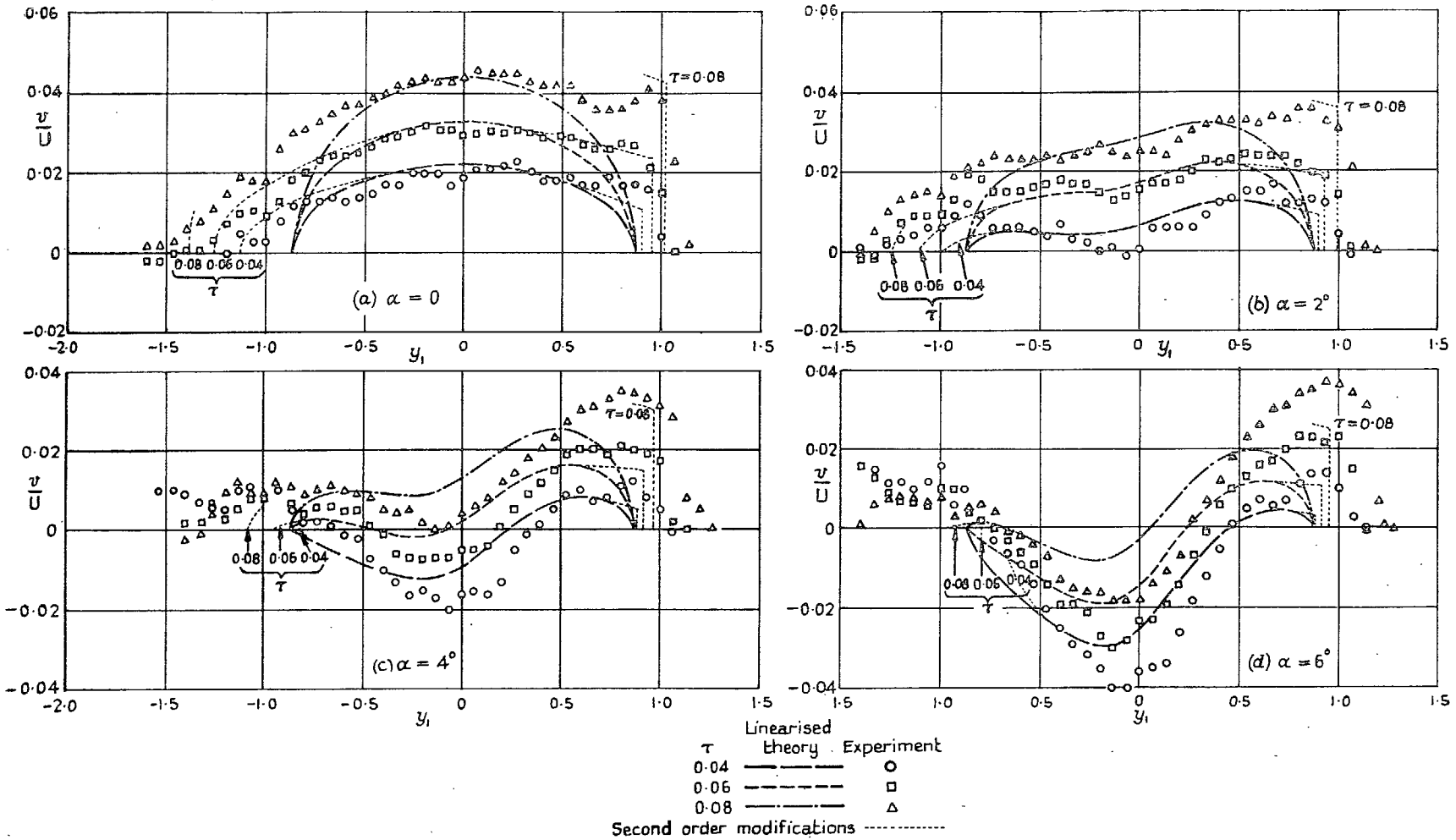

FIG. 13. Transverse component of velocity along the line $x = 0{\cdot}5$, $z = 0{\cdot}25$.

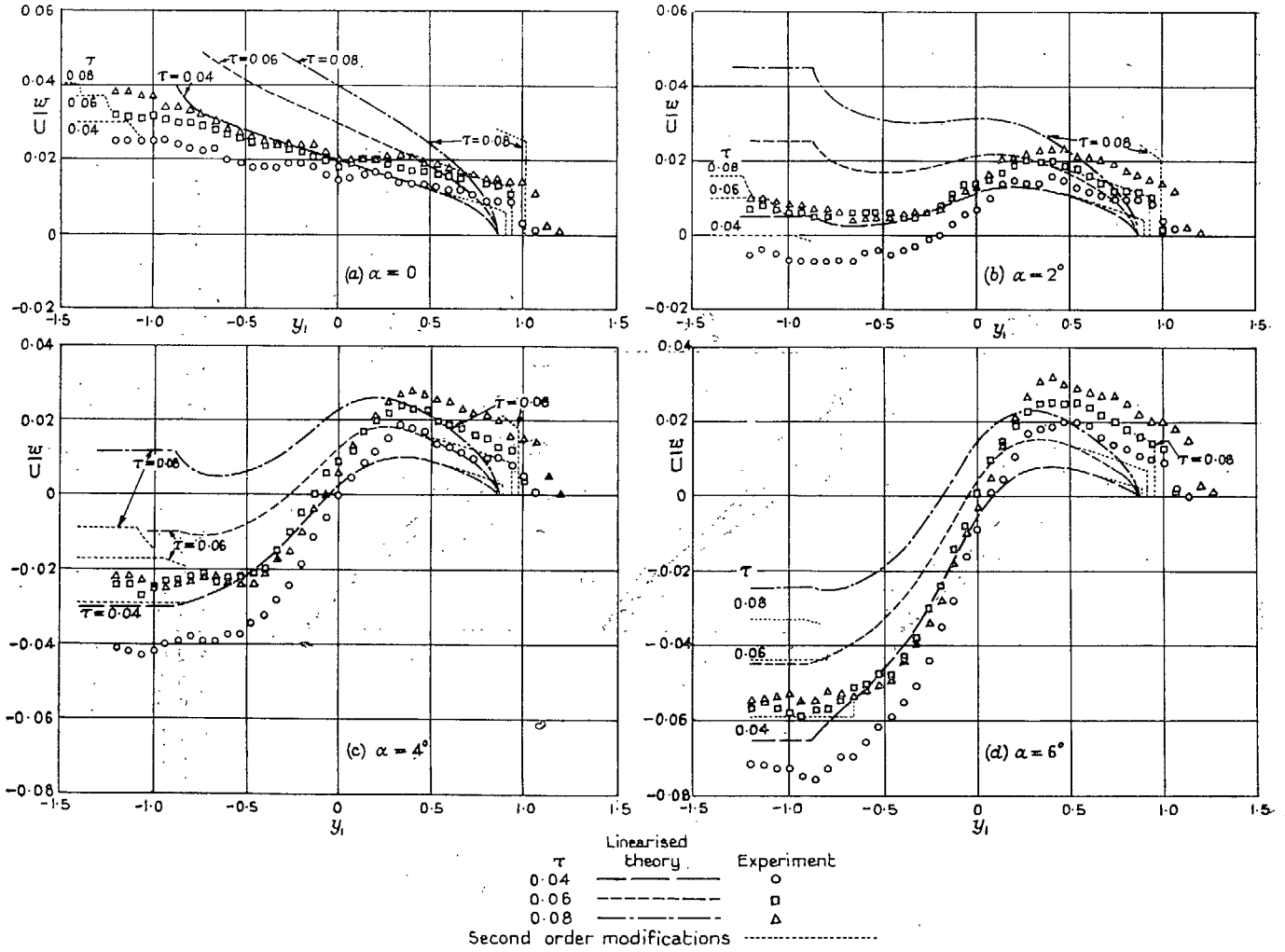

FIG. 14. Vertical component of velocity along the line $x = 0{\cdot}5$, $z = 0{\cdot}25$.

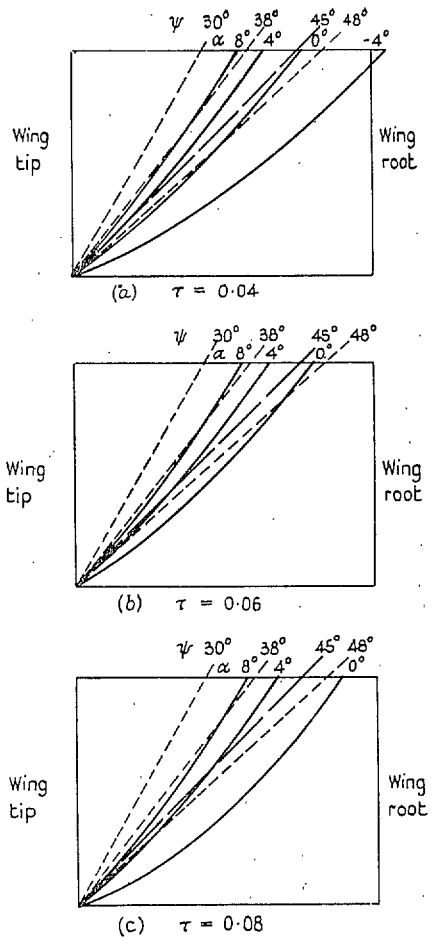

FIGS. 15a to 15c. Distortion of the tip region for rectangular biconvex wings. (Upper surface).

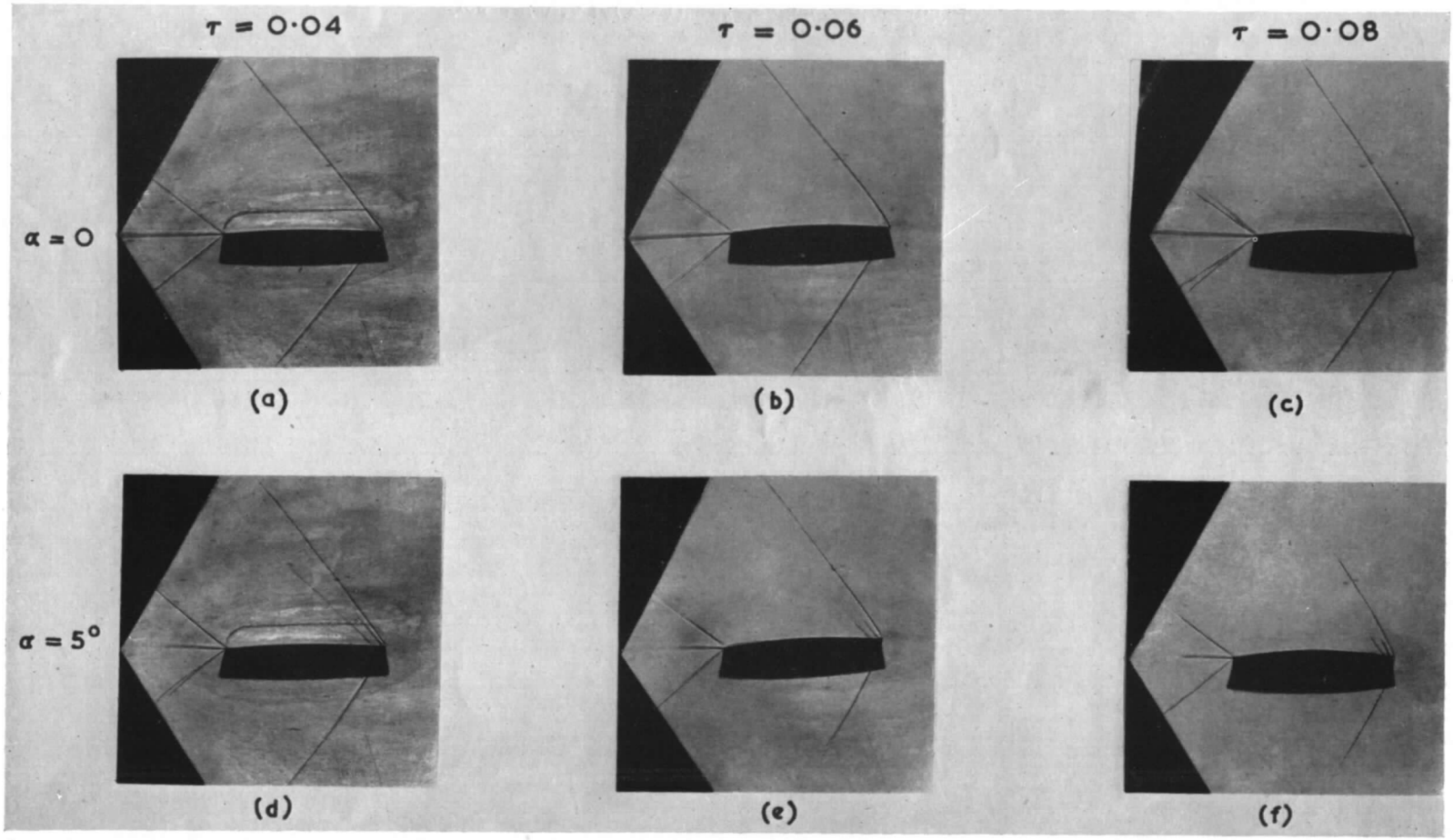

FIGS. 16(a) to 16(f). Direct shadow photographs.

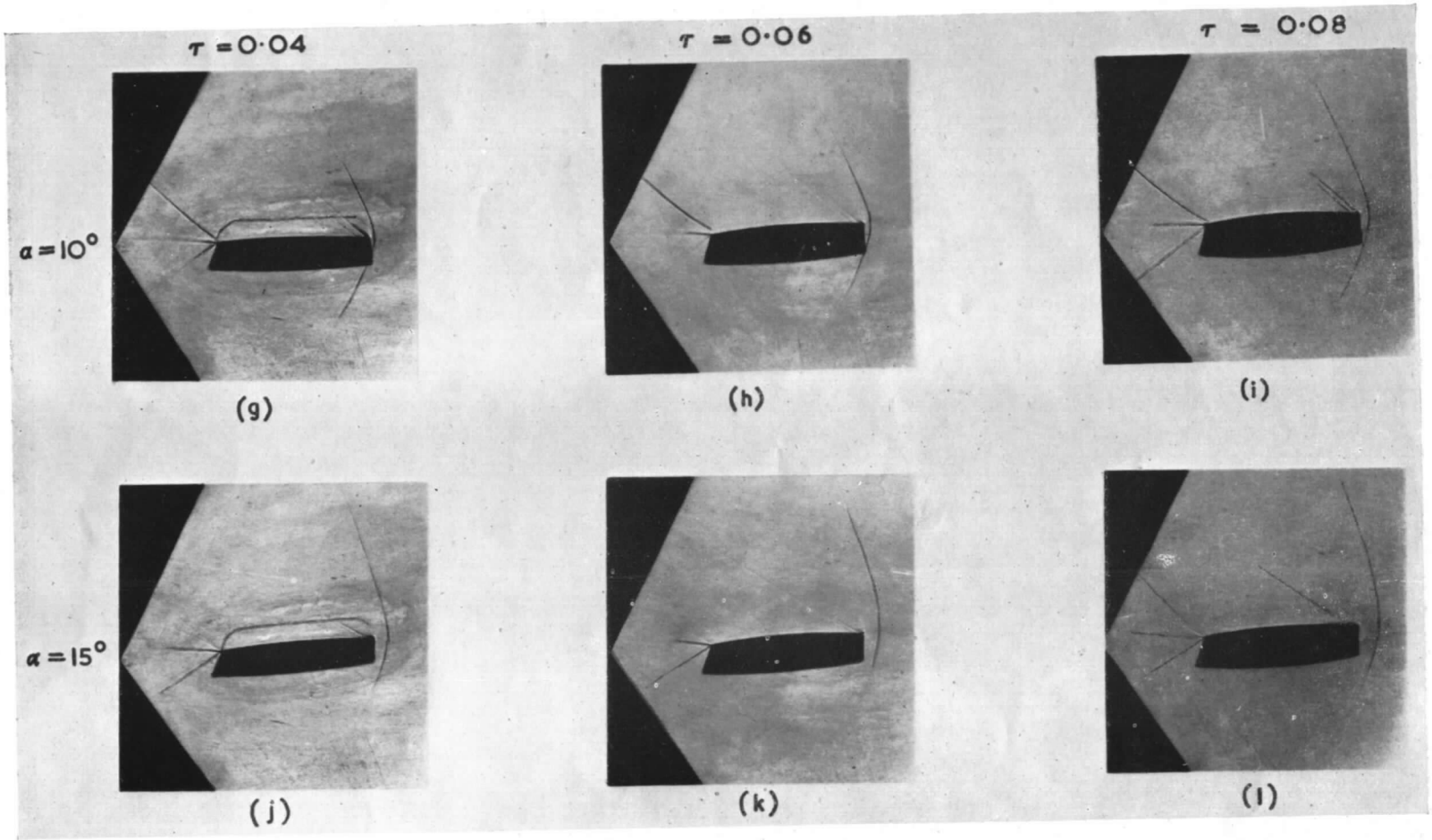

FIGS. 16(g) to 16(l). Direct shadow photographs.

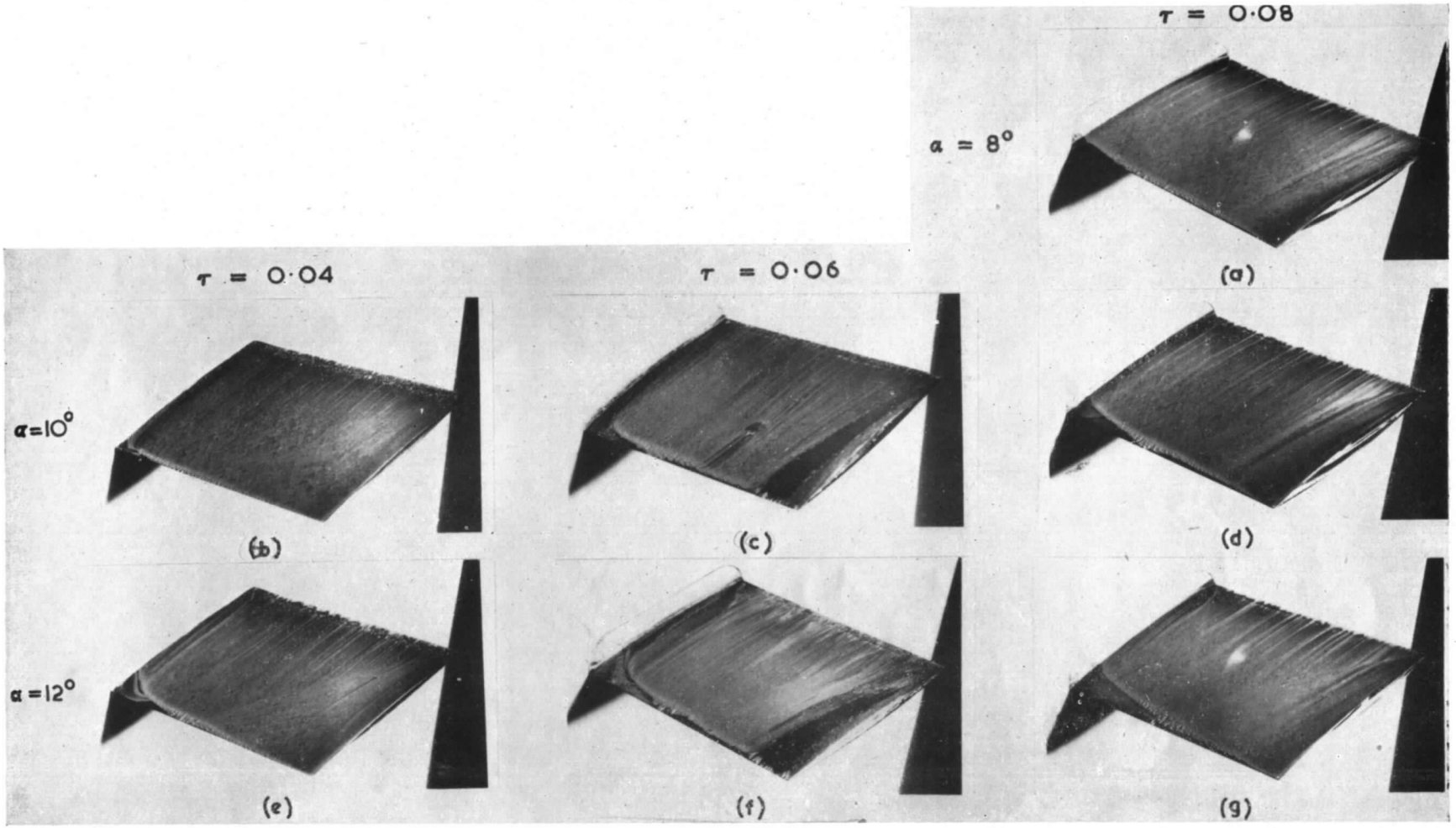

FIGS. 17(a) to 17(g). Surface flow patterns.

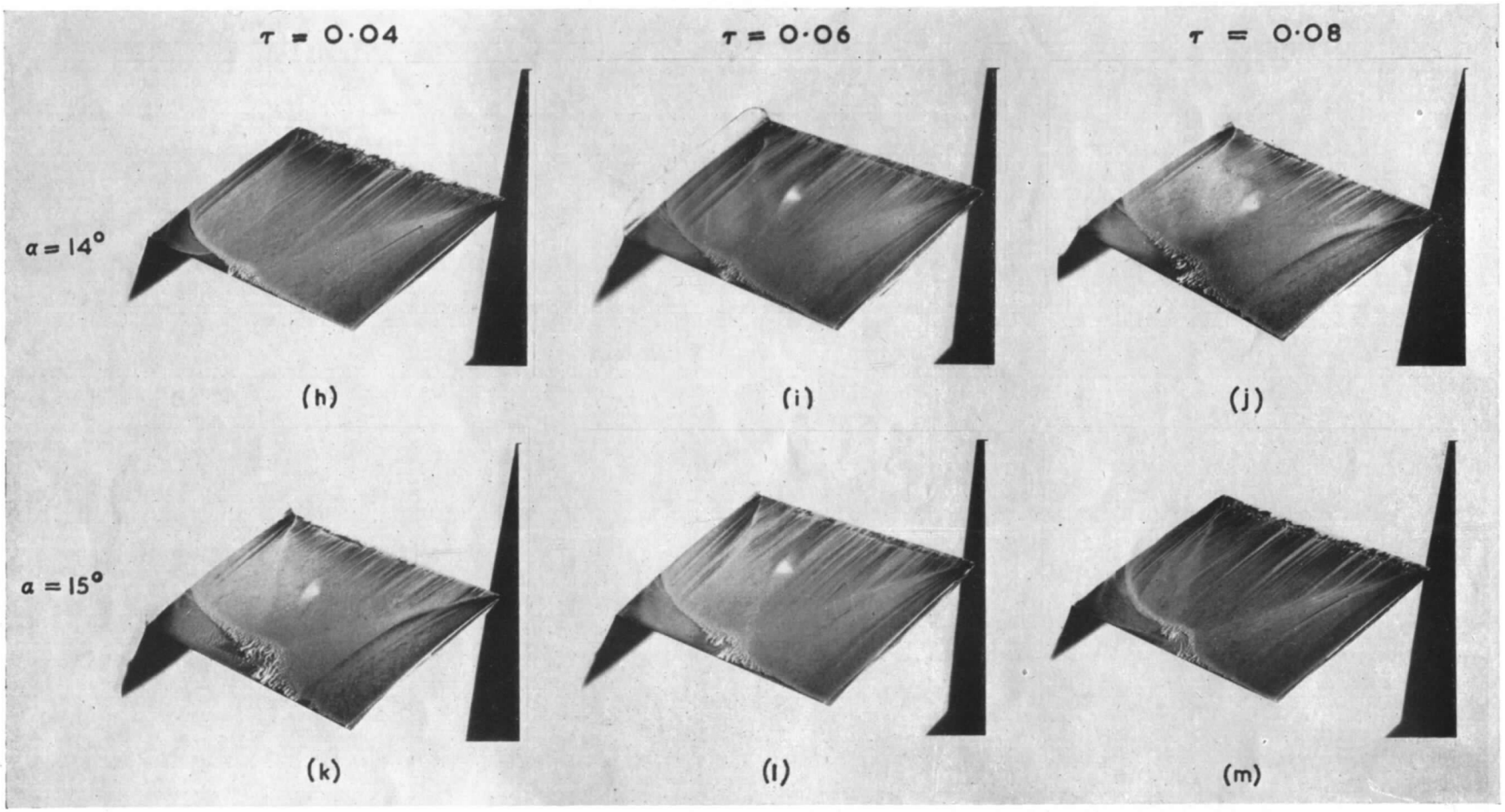

FIGS. 17(h) to 17(m). Surface flow patterns.

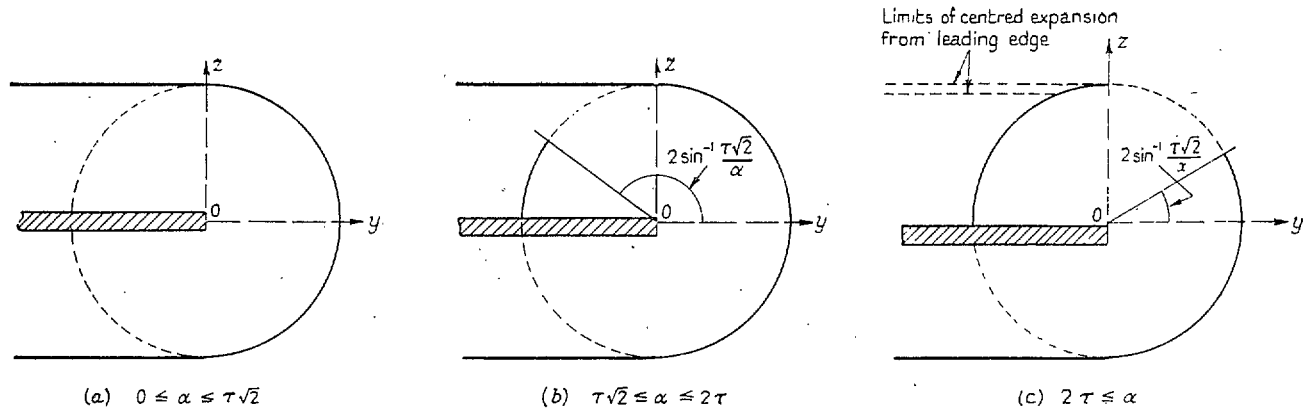

FIGS. 18a to 18c. Nature of leading-edge shock surface for a rectangular wedge of angle 4τ (diagrammatic).

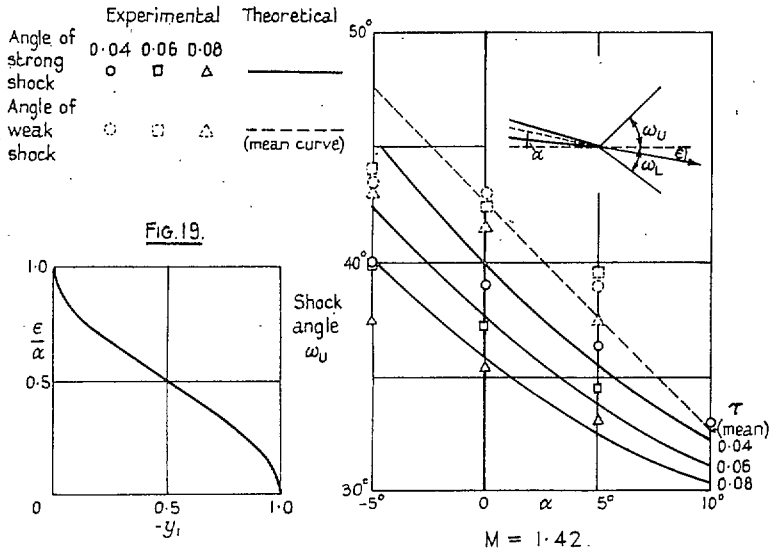

FIG. 19. Downwash at trailing-edge. (Linearised theory).

FIG. 20. Trailing-edge shock angle. (Upper surface).

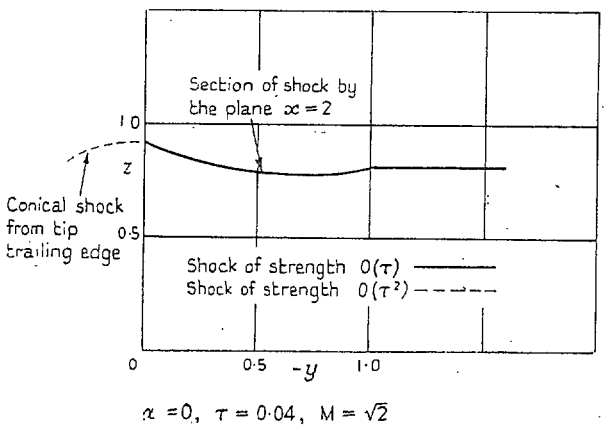

$\alpha = 0$, $\tau = 0{\cdot}04$, $M = \sqrt{2}$

FIG. 21. Shape of trailing-edge shock surface. (Linearised theory).

J4387 Wt.52/9843 K9 8/57 D&Co. 34/263

PRINTED IN GREAT BRITAIN

Publications of the Aeronautical Research Council

ANNUAL TECHNICAL REPORTS OF THE AERONAUTICAL RESEARCH COUNCIL (BOUND VOLUMES)

1939 Vol. I. Aerodynamics General, Performance, Airscrews, Engines. 50*s.* (52*s.*)
Vol. II. Stability and Control, Flutter and Vibration, Instruments, Structures, Seaplanes, etc. 63*s.* (65*s.*)

1940 Aero and Hydrodynamics, Aerofoils, Airscrews, Engines, Flutter, Icing, Stability and Control, Structures, and a miscellaneous section. 50*s.* (52*s.*)

1941 Aero and Hydrodynamics, Aerofoils, Airscrews, Engines, Flutter, Stability and Control, Structures. 63*s.* (65*s.*)

1942 Vol. I. Aero and Hydrodynamics, Aerofoils, Airscrews, Engines. 75*s.* (77*s.*)
Vol. II. Noise, Parachutes, Stability and Control, Structures, Vibration, Wind Tunnels. 47*s.* 6*d.* (49*s.* 6*d.*)

1943 Vol. I. Aerodynamics, Aerofoils, Airscrews. 80*s.* (82*s.*)
Vol. II. Engines, Flutter, Materials, Parachutes, Performance, Stability and Control, Structures. 90*s.* (92*s.* 9*d.*)

1944 Vol. I. Aero and Hydrodynamics, Aerofoils, Aircraft, Airscrews, Controls. 84*s.* (86*s.* 6*d.*)
Vol. II. Flutter and Vibration, Materials, Miscellaneous, Navigation, Parachutes, Performance, Plates and Panels, Stability, Structures, Test Equipment, Wind Tunnels. 84*s.* (86*s.* 6*d.*)

1945 Vol. I. Aero and Hydrodynamics, Aerofoils. 130*s.* (132*s.* 9*d.*)
Vol. II. Aircraft, Airscrews, Controls. 130*s.* (132*s.* 9*d.*)
Vol. III. Flutter and Vibration, Instruments, Miscellaneous, Parachutes, Plates and Panels, Propulsion. 130*s* (132*s.* 6*d.*)
Vol. IV. Stability, Structures, Wind tunnels, Wind Tunnel Technique. 130*s.* (132*s.* 6*d.*)

ANNUAL REPORTS OF THE AERONAUTICAL RESEARCH COUNCIL—

1937 2*s.* (2*s.* 2*d.*) 1938 1*s.* 6*d.* (1*s.* 8*d.*) 1939–48 3*s.* (3*s.* 5*d.*)

INDEX TO ALL REPORTS AND MEMORANDA PUBLISHED IN THE ANNUAL TECHNICAL REPORTS, AND SEPARATELY—

April, 1950 – – – – – R. & M. No. 2600. 2*s.* 6*d.* (2*s.* 10*d.*)

AUTHOR INDEX TO ALL REPORTS AND MEMORANDA OF THE AERONAUTICAL RESEARCH COUNCIL—

1909–January, 1954 – – – R. & M. No. 2570. 15*s.* (15*s.* 8*d.*)

INDEXES TO THE TECHNICAL REPORTS OF THE AERONAUTICAL RESEARCH COUNCIL—

December 1, 1936 — June 30, 1939. R. & M. No. 1850. 1*s.* 3*d.* (1*s.* 5*d.*)
July 1, 1939 — June 30, 1945. – R. & M. No. 1950. 1*s.* (1*s.* 2*d.*)
July 1, 1945 — June 30, 1946. – R. & M. No. 2050. 1*s.* (1*s.* 2*d.*)
July 1, 1946 — December 31, 1946. R. & M. No. 2150. 1*s.* 3*d.* (1*s.* 5*d.*)
January 1, 1947 — June 30, 1947. – R. & M. No. 2250. 1*s.* 3*d.* (1*s.* 5*d.*)

PUBLISHED REPORTS AND MEMORANDA OF THE AERONAUTICAL RESEARCH COUNCIL—

Between Nos. 2251–2349. – – R. & M. No. 2350. 1*s.* 9*d.* (1*s.* 11*d.*)
Between Nos. 2351–2449. – – R. & M. No. 2450. 2*s.* (2*s.* 2*d.*)
Between Nos. 2451–2549. – – R. & M. No. 2550. 2*s.* 6*d.* (2*s.* 10*d.*)
Between Nos. 2551–2649. – – R. & M. No. 2650. 2*s.* 6*d.* (2*s.* 10*d.*)
Between Nos. 2651–2749. – – R. & M. No. 5750. 2*s.* 6*d.* (2*s.* 10*d.*)

Prices in brackets include postage

HER MAJESTY'S STATIONERY OFFICE

York House, Kingsway, London W.C.2; 423 Oxford Street, London W.1;
13a Castle Street, Edinburgh 2; 39 King Street, Manchester 2; 2 Edmund Street, Birmingham 3; 109 St. Mary Street, Cardiff; Tower Lane, Bristol 1; 80 Chichester Street, Belfast, *or through any bookseller*

S.O. Code No. 23-3055